

Can the a.c.s. notion and the GLT theory handle approximated PDEs/FDEs with either moving or unbounded domains?

Andrea Adriani^{*1}, Alec Jacopo Almo Schiavoni-Piazza^{†2}, Stefano Serra-Capizzano^{‡1,3},
and Cristina Tablino-Possio^{§4}

¹Department of Science and High Technology, Division of Mathematics, University of Insubria, Via Valleggio 11, 22100 Como, Italy

²Scuola Internazionale Superiore di Studi Avanzati, Via Bonomea 265, 34136 Trieste, Italy

³Department of Information Technology, Division of Scientific Computing, Uppsala University, Box 337, SE-751 05, Uppsala, Sweden

⁴Department of Mathematics and Applications, University of Milano - Bicocca, via Cozzi, 53, 20125 Milano, Italy

Abstract

In the current note we consider matrix-sequences $\{B_{n,t}\}_n$ of increasing sizes depending on n and equipped with a parameter $t > 0$. For every fixed $t > 0$, we assume that each $\{B_{n,t}\}_n$ possesses a canonical spectral/singular values symbol f_t defined on $D_t \subset \mathbb{R}^d$ of finite measure, $d \geq 1$. Furthermore, we assume that $\{\{B_{n,t}\} : t > 0\}$ is an approximating class of sequences (a.c.s.) for $\{A_n\}$ and that $\bigcup_{t>0} D_t = D$ with $D_{t+1} \supset D_t$. Under such assumptions and via the notion of a.c.s., we prove results on the canonical distributions of $\{A_n\}$, whose symbol, when it exists, can be defined on the, possibly unbounded, domain D of finite or even infinite measure.

We then extend the concept of a.c.s. to the case where the approximating sequence $\{B_{n,t}\}_n$ has possibly a different dimension than the one of $\{A_n\}$. This concept seems to be particularly natural when dealing, e.g., with the approximation both of a partial differential equation (PDE) and of its (possibly unbounded, or moving) domain D , using an exhausting sequence of domains $\{D_t\}$.

Examples coming from approximated PDEs/FDEs with either moving or unbounded domains are presented in connection with the classical and the new notion of a.c.s., while numerical tests and a list of open questions conclude the present work.

Keywords Discretization of PDEs and FDEs, Unbounded domains, Spectral distribution of matrix-sequences, Approximating class of sequences, GLT theory.

^{*}andrea.adriani@uninsubria.it

[†]aschiavo@sissa.it

[‡]s.serracapizzano@uninsubria.it, stefano.serra@it.uu.se

[§]cristina.tablinopossio@unimib.it

1 Introduction

Partial Differential Equations (PDEs) and more recently Fractional Differential Equations (FDEs) represent standard tools employed for modeling real-world problems in Applied Sciences and Engineering. In particular, the notion of FDE can be considered as a generalization of that of PDE, in which fractional order derivatives are used describing anomalous diffusion processes stemming from concrete applications. The price to pay is the nonlocal nature of the underlying operators, which implies the dense character of the approximated equations and hence a higher computational cost.

In general, when considering either PDEs or FDEs, analytical solutions are not generally known in close form and when they are known via proper representation formulae, it happens that the related computation is costly. Indeed, while the analysis plays a fundamental role in establishing the well-posedness of a given PDE/FDE, numerical methods are crucial for an efficient computation of a numerical solution approximating the solution to the infinite dimensional problem within a certain error.

When using a linear numerical method and the given PDE/FDE is of linear type $Lu = g$ on some domain $\Omega \subset \mathbb{R}^\nu$, $\nu \geq 1$, we end up with a usually large linear system

$$A_n \mathbf{u}_n = \mathbf{g}_n, \quad (1)$$

where \mathbf{g}_n incorporate the approximation of the known term and the given boundary conditions and A_n is a square matrix of size d_n , $d_k < d_{k+1}$, $k \in \mathbb{N}$. In this way, as n tends to infinity, i.e. the matrix-size d_n tends to infinity, the approximated solution \mathbf{u}_n converges to the solution of the continuous problem $Lu = g$ in a given topology, depending on the continuous problem and on the given numerical method.

Looking at (1) collectively for every n , we observe that we are considering a whole sequence of linear systems with increasing matrix-size d_n . Hence it becomes useful to study the collective behavior of the sequence $\{A_n\}_n$ of coefficient matrices.

What is often observed in practice is that the sequence of matrices $\{A_n\}_n$ enjoys an asymptotic spectral distribution, which is somehow connected to the spectrum of the linear differential operator L associated either with the given PDE or with the given FDE. More in detail, for a large set of test functions F , usually for all continuous functions with bounded support or just continuous functions if the spectral norm of A_n is uniformly bounded by a constant independent of n , a weak-* convergence stands. More specifically, for every test function F , we have

$$\lim_{n \rightarrow \infty} \frac{1}{d_n} \sum_{j=1}^{d_n} F(\lambda_j(A_n)) = \frac{1}{\mu_m(D)} \int_D \frac{\sum_{i=1}^p F(\lambda_i(\mathbf{f}(\mathbf{y})))}{p} d\mathbf{y}, \quad (2)$$

where $\lambda_j(A_n)$, $j = 1, \dots, d_n$, are the eigenvalues of A_n , $\mu_m(\cdot)$ is the Lebesgue measure in \mathbb{R}^m , and $\lambda_i(\mathbf{f}(\mathbf{y}))$, $i = 1, \dots, p$, are the eigenvalues of a certain matrix-valued function

$$\mathbf{f} : D \subset \mathbb{R}^m \rightarrow \mathbb{C}^{p \times p}$$

with $\mu_m(D) \in (0, \infty)$. The function \mathbf{f} is referred to as the spectral symbol of the sequence of matrices $\{A_n\}$.

Informally speaking, relation (2) says that, for n large enough, the spectrum of A_n can be subdivided into p different subsets (or “branches”) of approximately the same cardinality d_n/p , and the i -th branch is approximately a uniform sampling over D of the i -th eigenvalue function $\lambda_i(\mathbf{f}(\mathbf{y}))$, $i = 1, \dots, p$. In particular, the number r coincides with the number of “branches” that compose the spectrum of A_n . For instance, if $k = 1$, $d_n = np$, and $D = [a, b]$, then up to few possible outliers the eigenvalues of A_n are approximately equal to

$$\lambda_i \left(\mathbf{f} \left(a + j \frac{b-a}{n} \right) \right), \quad j = 1, \dots, n, \quad i = 1, \dots, p;$$

if $k = 2$, $d_n = n^2 p$, and $D = [a_1, b_1] \times [a_2, b_2]$, then again up to few possible outliers the eigenvalues of A_n are approximately equal to

$$\lambda_i \left(\mathbf{f} \left(a_1 + j_1 \frac{b_1 - a_1}{n}, a_2 + j_2 \frac{b_2 - a_2}{n} \right) \right), \quad j_1, j_2 = 1, \dots, n, \quad i = 1, \dots, p;$$

and so on in a m -dimensional setting, with $m > 2$ integer.

A complementary notion is that of singular value symbol and singular value distribution. For this further notion, instead of (2), for every test function F , we have

$$\lim_{n \rightarrow \infty} \frac{1}{d_n} \sum_{j=1}^{d_n} F(\sigma_j(A_n)) = \frac{1}{\mu_m(D)} \int_D \frac{\sum_{i=1}^p F(\sigma_i(\mathbf{f}(\mathbf{y})))}{p} d\mathbf{y},$$

where $\sigma_j(A_n)$, $j = 1, \dots, d_n$, are the singular values of A_n , $\sigma_i(\mathbf{f}(\mathbf{y}))$, $i = 1, \dots, p$, are the singular values of a certain matrix-valued function $\mathbf{f} : D \subset \mathbb{R}^m \rightarrow \mathbb{C}^{p \times p}$ with $\mu_m(D) \in (0, \infty)$ and where the informal meaning exactly mirrors that described above for the spectral symbol. The function \mathbf{f} is referred to as the singular value symbol of the sequence of matrices $\{A_n\}$.

It is then clear that the spectral symbol (singular value symbol) \mathbf{f} provides a “compact” and quite accurate description of the spectrum (singular values) of the discretization matrices A_n . The identification and the study of the symbol are consequently two important steps in the analysis of A_n and, as a consequence, in the analysis and in the design of fast iterative solvers for the linear systems in (1), especially for large matrix-sizes d_n .

We remind that this type of eigenvalue distribution results are studied since the beginning of the last century in the context of the sequences of Toeplitz matrices generated by real-valued (or Hermitian-valued) functions, as the reader can check in the papers [45, 47, 48] or in the books [7, 20, 21], taking into account related references therein. Wide generalizations to the $*$ -algebras of GLT matrix-sequences are considered in [20, 21, 3, 4] with specific applications to the approximation via local numerical methods of (systems of) PDEs/FDEs also with nonsmooth variable coefficients and irregular but bounded domains/manifolds [1, 12, 13, 14, 16, 17, 18, 23, 19, 29, 28].

For giving a global picture, despite the great variety of numerical techniques, the parameters in formula (2) in the GLT analysis depend on a combination of the continuous PDE problem and of the approximation technique. For instance, the typical D is $\Omega \times [-\pi, \pi]^\nu$, if Ω is a domain in \mathbb{R}^ν of positive and finite Lebesgue measure, where the PDE under consideration is defined; see the early Locally Toeplitz and GLT papers [41, 42, 44]. As a consequence, the typical m equals 2ν while, and this is natural, in the case of a submanifold of co-dimension c , we have $m = 2(\nu - c)$, $1 \leq c \leq \nu - 1$. The parameter $p = s\alpha(d)$ ($d = \nu$ or $\nu - c$ in the submanifold setting), where s is the size of the vector function g in the continuous equation $Lu = g$: in the case of a vector PDE obviously we have $s > 1$. More interestingly $\alpha(d)$ depends very much on the approximation scheme, in general of local type, such as Finite Elements [8], Discontinuous Galerkin [24], Finite Differences [43], Finite Volumes [50], Isogeometric Analysis [9] etc. More precisely, in the case of Finite Differences [41], Finite Volumes [14], Isogeometric Analysis of degree k and maximal regularity $k - 1$ [13], Finite Elements of degree 1 [5], we have $\alpha(d) = 1$, while for Isogeometric Analysis of intermediate regularity l with $l < k - 1$, we observe $\alpha(d) = (k - l)^d$ [23]. In the case of Finite Elements of higher order k , we have $\alpha(d) = k^d$ [22, 34], while when using Discontinuous Galerkin $\alpha(d) = (k + l)^d$ [17]. Notice that the latter two formulas are a special instance of $\alpha(d) = (k - l)^d$, since $l = 0$ in the Finite Elements of high order and $l = -1$ in the DG setting, because of the global discontinuity. We also remark that the exponential growth of the type $\alpha(d) = (k - l)^d$ is a drawback from a spectral viewpoint because only one branch of the spectrum is acoustic, that is related to the spectrum of the continuous operator, while the remaining very numerous branches are optical, in the sense that they behave like a pathology introduced by the numerical method (see e.g. [10] and references therein), and in addition they represent a challenge for designing fast iterative solvers, due to the very involved structure of the spectrum (see the applications in [3, 4, 19, 20, 21, 23]).

The paper is organized as follows. Sections 2 and 3 are devoted to introduce some notation and basic tools, such as the concept of spectral distribution, approximating class of sequences and Toeplitz matrix-sequences. Section 4 contains the main approximation results. In particular, in Subsection 4.1, we introduce the new tool of generalized approximating class of sequences (g.a.c.s.) and we give an approximation result which highlights its usefulness. In Section 5 we give few application for constant coefficient PDEs, complemented by numerical experiments and related visualizations, which are then extended to the case of variable coefficients in Section ?? . Finally, Section 7 is devoted to concluding remarks and to mention few open problems and future directions of research.

2 Spectral distribution and Approximating class of sequences

In this section we introduce the tools of spectral distribution for a matrix sequence and of approximating class of sequences (a.c.s.), which is a fruitful concept in the theory of numerical approximation and asymptotic spectral analysis of matrix-sequences. We start with the definitions and then recall some useful results connecting the two concepts.

Definition 2.1. Let $\{A_n\}_n$ be a matrix-sequence and let $f : D \rightarrow \mathbb{C}^{p_1 \times p_2}$ be a measurable Hermitian matrix-valued function defined on the measurable (bounded) set $D \subset \mathbb{R}^m$, with $0 < \mu_m(D) < \infty$. We write that $\{A_n\}_n$ is distributed as f in the sense of singular values in D and we write $\{A_n\}_n \sim_\sigma (f, D)$, if

$$\lim_{n \rightarrow \infty} \sum_{j=1}^{d_n \wedge d'_n} \frac{F(\sigma_j(A_n))}{d_n \wedge d'_n} = \frac{1}{\mu(D)} \int_D \sum_{k=1}^p \frac{F(\sigma_k(f(s)))}{p} ds, \quad \forall F \in C_c(\mathbb{R}),$$

where $\sigma_1(f(s)), \dots, \sigma_p(f(s))$ are the singular values of $f(s)$, $p = p_1 \wedge p_2$. We call f the singular value symbol of $\{A_n\}_n$.

With the same notation as before, imposing $d_n = d'_n$, we write that $\{A_n\}_n$ is distributed as f in the sense of eigenvalues in D with necessarily $p_1 = p_2 = p$ and we write $\{A_n\}_n \sim_\lambda (f, D)$, if

$$\lim_{n \rightarrow \infty} \sum_{j=1}^{d_n} \frac{F(\lambda_j(A_n))}{d_n} = \frac{1}{\mu(D)} \int_D \sum_{k=1}^p \frac{F(\lambda_k(f(s)))}{p} ds, \quad \forall F \in C_c(\mathbb{R}),$$

where $\lambda_1(f(s)), \dots, \lambda_p(f(s))$ are the eigenvalues of $f(s)$. We call f the spectral symbol of $\{A_n\}_n$.

Definition 2.2. Let $\{A_n\}_n$ be a matrix-sequence of size $d_n \times d'_n$ with d_n and d'_n monotonically increasing integer sequences and let $\{\{B_{n,t}\}_t\}_n$ be a sequence of matrix-sequences of the same size $d_n \times d'_n$. We say that $\{\{B_{n,t}\}_t\}_n$ is an approximating class of sequences (a.c.s.) for $\{A_n\}_n$ if the following condition is met: for every t there exists n_t such that, for $n > n_t$,

$$A_n = B_{n,t} + R_{n,t} + N_{n,t}, \quad \text{rank}(R_{n,t}) \leq c(t)d_n \wedge d'_n,$$

$$\|N_{n,t}\| \leq \omega(t),$$

where $n_t, c(t), \omega(t)$ depend only on t , and

$$\lim_{t \rightarrow \infty} c(t) = \lim_{t \rightarrow \infty} \omega(t) = 0.$$

The following theorem constitutes a link between a.c.s. and spectral distribution.

Theorem 2.1. Let $\{A_n\}_n$ be a matrix-sequence of size $d_n \times d'_n$ with d_n and d'_n monotonically increasing integer sequences and let $\{\{B_{n,t}\}_t\}_n$ be an a.c.s. for $\{A_n\}_n$. Suppose that $\{\{B_{n,t}\}_t\}_n \sim_\sigma (f_t, D)$ and f_t converges in measure to f , then $\{A_n\}_n \sim_\sigma (f, D)$. Furthermore, if $d_n = d'_n$, all the involved matrices are Hermitian, and $\{\{B_{n,t}\}_t\}_n \sim_\lambda (f_t, D)$ and f_t converges in measure to f , then $\{A_n\}_n \sim_\lambda (f, D)$

The tool is quite powerful and it was introduced in the seminal work by Tilli [44] on locally Toeplitz matrix-sequences. Then in [40] the terminology was provided and further results were given. An account of the general theory on generalized Locally Toeplitz (GLT) matrix-sequences, based on the a.c.s. notion, can be found in [3, 4, 20, 21, 23] and references therein.

In these books and long research/exposition papers one can find also examples of applications ranging from approximated integro-differential equations, approximated partial differential equations, approximated fractional differential equations with any kind of methods (finite elements, finite differences, isogeometric analysis, finite volumes etc) and with very mild assumptions: only Riemann integrability in the case of variable coefficients, only Peano-Jordan measurability of the domain (see e.g. [26] for the latter two notions), grids approximated by a given function applied on uniform grids. In particular the richness in the potential domains is obtained via the notion of reduced GLT matrix sequences: see [41][pp. 395–399] for a detailed example, [42][Section 3.1.4] for a initial proposal and related terminology, and the long dense paper [2] for a systematic treatment of the subject and for a complete theoretical development.

However, in all cases the idea is the immersion of the given Peano-Jordan measurable domain into a cube or rectangle in the appropriate number of dimensions, where this idea is related to the immersed methods [11, 27] and to the less recent idea of fictitious domains [25, 30]. The reader is referred also to [18, 31] for an asymptotical analysis and numerical methods regarding standard PDEs and fractional PDEs using the immersion idea and the reduced GLT tools.

However, the previous techniques are not applicable in the case of unbounded domain. The theorems in the present paper and the applications in Section 5 and ?? fill the gap and complete the picture, by considering moving and unbounded domains with either finite or infinite Lebesgue measure. Here, the basic a.c.s. and the new g.a.c.s. notions are the main tools which allow us to go beyond the GLT machinery. The new g.a.c.s. concept allows to deal with matrix-sequences defined by different sequences of dimensions and this may happen e.g. in several approximation schemes for differential equations. The idea is already present in [29] in Theorem 4.3, Corollary 4.4 and it is reminiscent of the extradimensional approach proposed by Tyrtshnikov more than two decades ago (see again [29], beginning of Section 4.2).

3 Multi-index notation, Toeplitz and multi-level Toeplitz matrices

In this section, we first introduce a multi-index notation that we use hereafter. Given an integer $d \geq 1$, a d -index \mathbf{k} is an element of \mathbb{Z}^d , that is, $\mathbf{k} = (k_1, \dots, k_d)$ with $k_r \in \mathbb{Z}$ for every $r = 1, \dots, d$. We intend \mathbb{Z}^d equipped with the standard lexicographic ordering, that is, given two d -indices $\mathbf{i} = (i_1, \dots, i_d)$, $\mathbf{j} = (j_1, \dots, j_d)$, we write $\mathbf{i} \triangleleft \mathbf{j}$ if $i_r < j_r$ for the first $r = 1, 2, \dots, d$ such that $i_r \neq j_r$. The relations $\trianglelefteq, \triangleright, \trianglerighteq$ are defined accordingly.

Given two d -indices \mathbf{i}, \mathbf{j} , we write $\mathbf{i} < \mathbf{j}$ if $i_r < j_r$ for every $r = 1, \dots, d$. The relations $\leq, >, \geq$ are defined accordingly.

We use bold letters for vectors and vector/matrix-valued functions. We indicate with $\mathbf{0}, \mathbf{1}, \mathbf{2}, \dots$, the d -dimensional constant vectors $(0, 0, \dots, 0), (1, 1, \dots, 1), (2, 2, \dots, 2), \dots$, respectively. With the notation $\frac{\mathbf{i}}{\mathbf{n}}$ we mean the element-wise division of vectors, i.e., $\frac{\mathbf{i}}{\mathbf{n}} = \left(\frac{i_1}{n_1}, \dots, \frac{i_d}{n_d}\right)$. We write $|\mathbf{i}|$ for the vector $(|i_1|, \dots, |i_d|)$. Finally, given a d -index \mathbf{n} , we write $\mathbf{n} \rightarrow \infty$ meaning that $\min_{r=1, \dots, d} \{n_r\} \rightarrow \infty$.

A Toeplitz matrix of order n is characterized by the fact that all the diagonals are constant: $(T_n)_{i,j} =$

t_{i-j} for $i, j = 1, \dots, n$ and some coefficients t_k , $k = 1 - n, \dots, n - 1$:

$$T_n = \begin{pmatrix} t_0 & t_{-1} & \cdots & t_{1-n} \\ t_1 & t_0 & \ddots & \vdots \\ \vdots & \ddots & \ddots & t_{-1} \\ t_{n-1} & \cdots & t_1 & t_0 \end{pmatrix}.$$

When every term t_k is a matrix of fixed size $p_1 \times p_2$, we say that T_n is of block Toeplitz type. The definition of d -level Toeplitz matrices is more involved and it is based on the following recursive idea: a d -level Toeplitz matrix is a Toeplitz matrix where each coefficient t_k is a $(d-1)$ -level Toeplitz matrix and so on. Using standard multi-index notation, we can give a more detailed definition as follows: a d -level Toeplitz matrix is a matrix $T_{\mathbf{n}}$ such that

$$T_{\mathbf{n}} = (\mathbf{t}_{i-j})_{i,j=1}^{\mathbf{n}} \in \mathbb{C}^{(n_1 \cdots n_d) \times (n_1 \cdots n_d)},$$

with the multi-index \mathbf{n} such that $\mathbf{0} < \mathbf{n} = (n_1, \dots, n_d)$ and $\mathbf{t}_{\mathbf{k}} \in \mathbb{C}$, $-(\mathbf{n} - \mathbf{1}) \leq \mathbf{k} \leq \mathbf{n} - \mathbf{1}$. If the basic element $t_{\mathbf{k}}$ is a block of fixed size $p_1 \times p_2$, $\max\{p_1, p_2\} \geq 2$, we write that the matrix is a d -level block Toeplitz matrix and we denote it by $T_{\mathbf{n}, p_1, p_2}$:

$$T_{\mathbf{n}, p_1, p_2} = (\mathbf{t}_{i-j})_{i,j=1}^{\mathbf{n}} \in \mathbb{C}^{(n_1 \cdots n_d p_1) \times (n_1 \cdots n_d p_2)}, \quad \mathbf{t}_{\mathbf{k}} \in \mathbb{C}^{p_1 \times p_2}.$$

Given now a function $\mathbf{f} : [-\pi, \pi]^d \rightarrow \mathbb{C}^{p_1 \times p_2}$ in $L^1([-\pi, \pi]^d)$, we denote its Fourier coefficients by

$$\hat{\mathbf{f}}_{\mathbf{k}} = \frac{1}{(2\pi)^d} \int_{[-\pi, \pi]^d} \mathbf{f}(\boldsymbol{\theta}) e^{-i \mathbf{k} \cdot \boldsymbol{\theta}} d\boldsymbol{\theta} \in \mathbb{C}^{p_1 \times p_2}, \quad \mathbf{k} \in \mathbb{Z}^d, \quad \mathbf{k} \cdot \boldsymbol{\theta} = \sum_{r=1}^d k_r \theta_r,$$

(the integrals are done component-wise), and we associate to \mathbf{f} the family of d -level block Toeplitz matrices

$$T_{\mathbf{n}, p_1, p_2}(\mathbf{f}) := (\hat{\mathbf{f}}_{i-j})_{i,j=1}^{\mathbf{n}}, \quad \mathbf{n} \in \mathbb{N}^d.$$

In this context, \mathbf{f} is called the generating function of the sequence $\{T_{\mathbf{n}, p_1, p_2}\}$.

The following result links the definition of symbol function and generating function for Toeplitz matrix-sequences.

Theorem 3.1 ([45, 46, 15]). *Let $\mathbf{f} : [-\pi, \pi]^d \rightarrow \mathbb{C}^{p_1 \times p_2}$ be a function belonging to $L^1([-\pi, \pi]^d)$, $p_1, p_2, d \geq 1$. Then*

$$\{T_{\mathbf{n}, p_1, p_2}(\mathbf{f})\}_{\mathbf{n}} \sim_{\sigma} \mathbf{f},$$

that is the generating function of $\{T_{\mathbf{n}, p_1, p_2}(\mathbf{f})\}_{\mathbf{n}}$ coincides with its singular value symbol. When $p_1 = p_2 = p$ and \mathbf{f} is Hermitian-valued almost everywhere or belongs to the Tilli class, i.e. \mathbf{f} is essentially bounded, the closure of its range has empty interior, and the range does not disconnect the complex field (see [46] when $p = 1$ and [15] when $p > 1$), we have

$$\{T_{\mathbf{n}, p, p}(\mathbf{f})\}_{\mathbf{n}} \sim_{\lambda} \mathbf{f},$$

that is the generating function of $\{T_{\mathbf{n}, p, p}(\mathbf{f})\}_{\mathbf{n}}$ coincides with its spectral symbol. Here, when $p_1 = p_2 = p$, for range of \mathbf{f} we mean the union of the ranges of the p eigenvalue functions of \mathbf{f} .

4 Main results

We start this section by stating and proving a theorem which extends the practical purposes of the a.c.s. notion to the case of unbounded domains, possibly of infinite measure, using exhaustions by bounded sets of finite measure.

Theorem 4.1. *Let $\{A_n\}$ be a matrix-sequence with A_n of size $d_n \times d'_n$ with d_n and d'_n monotonically increasing integer sequences. Let D be a measurable set in \mathbb{R}^d for some $d \geq 1$, possibly unbounded and of infinite measure and let $f : D \rightarrow \mathbb{C}^{p_1 \times p_2}$, $p_1, p_2 \geq 1$, be a measurable function with $p = p_1 \wedge p_2$. Let D_t be an exhaustion of D , that is, $D_{t+1} \supset D_t$ for every $t > 0$ and $\bigcup_{t>0} D_t = D$. Assume that $\exists \{B_{n,t}\}$ such that $\{\{B_{n,t}\} : t > 0\}$ is an a.c.s. for $\{A_n\}$ with $\{B_{n,t}\} \sim_\sigma (f_t, D_t)$, i.e.,*

$$\lim_{n \rightarrow \infty} \sum_{j=1}^{d_n \wedge d'_n} \frac{F(\sigma_j(B_{n,t}))}{d_n \wedge d'_n} = \frac{1}{\mu(D_t)} \int_{D_t} \sum_{k=1}^p \frac{F(\sigma_k(f_t(s)))}{p} ds = \alpha_t(F)$$

for every $F \in C_c(\mathbb{R})$. Assume that, for every $F \in C_c(\mathbb{R})$,

$$\lim_{t \rightarrow \infty} \alpha_t(F) = \alpha(F).$$

Then

$$\lim_{n \rightarrow \infty} \sum_{j=1}^{d_n \wedge d'_n} \frac{F(\sigma_j(A_n))}{d_n \wedge d'_n} = \alpha(F). \quad (3)$$

If in addition we have

$$\lim_{t \rightarrow \infty} f_t^E = f \quad (4)$$

in D almost everywhere, with

$$f_t^E = \begin{cases} f_t(s) & \text{if } s \in D_t \\ 0 & \text{otherwise,} \end{cases}$$

then we write $\{A_n\} \sim_{\sigma, \text{moving}} (f, D)$. Moreover, if $\mu(D) < \infty$, we have

$$\alpha(F) = \frac{1}{\mu(D)} \int_D \sum_{k=1}^p \frac{F(\sigma_k(f(s)))}{p} ds.$$

Proof. By the assumption $\{B_{n,t}\} \sim (f_t, D_t)$ we know that $\mu(D_t) > 0$ and hence, since $D \supset D_t$ for every $t > 0$, we deduce that $\mu(D) > 0$.

First, we note that relation (6) is true if and only if it is true for any F in C^1 with bounded support by simple functional approximation techniques. At this point, taking $F = F^\uparrow + F^\downarrow$, with $F^\uparrow(x) = \int_0^x (F')^+(t) dt$ and $F^\downarrow(x) = \int_0^x (F')^-(t) dt$, where $g^+ = \max(g, 0)$ and $g^- = \max(-g, 0)$, we deduce by linearity that (6) is true if and only if it holds for every G continuous, differentiable (with G' nonnegative), being equal to 0 for every $x \leq c_1$ and being constant (equal to $\|G\|_\infty$) for every $x \geq c_2$. Now, since $\{\{B_{n,t}\} : t > 0\}$ is an a.c.s. for $\{A_n\}$, we deduce that $\exists s(n, t) \leq \alpha(t)(d_n \wedge d'_n)$ for which

$$\sigma_{j+\alpha(t)(d_n \wedge d'_n)}(B_{n,t}) - \frac{1}{t} \leq \sigma_j(A_n) \leq \sigma_{j-\alpha(t)(d_n \wedge d'_n)}(B_{n,t}) + \frac{1}{t}, \quad (5)$$

where $\lim_{t \rightarrow \infty} \alpha(t) = 0$ and $j - \alpha(t)(d_n \wedge d'_n)$ has to be intended equal to 1 if $j - \alpha(t)(d_n \wedge d'_n) \leq 1$ and it has to be intended equal to $d_n \wedge d'_n$ if $j - \alpha(t)(d_n \wedge d'_n) \geq d_n \wedge d'_n$. Inequalities in (5), together with

the features of G , lead to

$$\begin{aligned} \frac{1}{d_n \wedge d'_n} \sum_{j=1}^{d_n \wedge d'_n} G\left(\sigma_j(B_{n,t}) - \frac{1}{t}\right) - \|G\|_\infty \alpha(t) &\leq \\ &\leq \frac{1}{d_n \wedge d'_n} \sum_{j=1}^{d_n \wedge d'_n} G(\sigma_j(A_n)) \leq \frac{1}{d_n \wedge d'_n} \sum_{j=1}^{d_n \wedge d'_n} G\left(\sigma_j(B_{n,t}) + \frac{1}{t}\right) + \|G\|_\infty \alpha(t). \end{aligned}$$

Since

$$G\left(x + \frac{1}{t}\right) \leq G(x) + \|G'\|_\infty \frac{1}{t} \quad \text{and} \quad G\left(x - \frac{1}{t}\right) \geq G(x) - \|G'\|_\infty \frac{1}{t}$$

we conclude that

$$\begin{aligned} \frac{1}{d_n \wedge d'_n} \sum_{j=1}^{d_n \wedge d'_n} G(\sigma_j(B_{n,t})) - \frac{1}{t} \|G'\|_\infty - \|G\|_\infty \alpha(t) &\leq \\ &\leq \frac{1}{d_n \wedge d'_n} \sum_{j=1}^{d_n \wedge d'_n} G(\sigma_j(A_n)) \leq \frac{1}{d_n \wedge d'_n} \sum_{j=1}^{d_n \wedge d'_n} G(\sigma_j(B_{n,t})) + \frac{1}{t} \|G'\|_\infty + \|G\|_\infty \alpha(t). \end{aligned}$$

Since

$$\lim_{t \rightarrow \infty} \frac{1}{t} \|G'\|_\infty \pm \alpha(t) \|G\|_\infty = 0,$$

taking any $\varepsilon > 0$ there exists $n_\varepsilon = n_{\varepsilon, t, G}$ such that for every $n \geq n_\varepsilon$ we have

$$\frac{1}{d_n \wedge d'_n} \sum_{j=1}^{d_n \wedge d'_n} G(\sigma_j(A_n)) \in \left[\alpha_t(G) - \frac{\varepsilon}{2}, \alpha_t(G) + \frac{\varepsilon}{2} \right] \subseteq [\alpha(G) - \varepsilon, \alpha(G) + \varepsilon].$$

This concludes the first part of the theorem.

For the in addition part, we observe that under the assumption $\mu(D) < \infty$, we have $\lim_{t \rightarrow \infty} \mu(D_t) = \mu(D)$ and $\lim_{t \rightarrow \infty} \mu(D \setminus D_t) = 0$. Using Equation (7), it follows that

$$\begin{aligned} \lim_{t \rightarrow \infty} \int_{D_t} \frac{\sum_{k=1}^p F(\sigma_k(f_t(s)))}{p} ds &= \lim_{t \rightarrow \infty} \left(\int_D \frac{\sum_{k=1}^p F(\sigma_k(f_t^E(s)))}{p} ds - F(0) \mu(D \setminus D_t) \right) \\ &= \int_D \frac{\sum_{k=1}^p F(\sigma_k(f(s)))}{p} ds, \end{aligned}$$

ending the proof. \square

Under the hypothesis that the sequences are constituted by Hermitian matrices, we can extend the previous result to the case of eigenvalues by obtaining the theorem below. The proof is an eigenvalue version of the proof of Theorem 4.1: the steps are identical and we leave them to the interested reader.

Theorem 4.2. *Let $\{A_n\}$ be a matrix-sequence with A_n of order d_n such that $A_n = A_n^*$ with d_n and monotonically increasing integer sequence. Let D be a measurable set in \mathbb{R}^d for some $d \geq 1$, possibly unbounded and of infinite measure and let $f : D \rightarrow \mathbb{C}^{p \times p}$, $p \geq 1$, be a measurable function. Let D_t be an exhaustion of D , that is, $D_{t+1} \supset D_t$ for every $t > 0$ and $\bigcup_{t>0} D_t = D$. Assume that $\exists \{B_{n,t}\}$ such that $B_{n,t} = B_{n,t}^*$ for every n, t and that $\{\{B_{n,t}\} : t > 0\}$ is an a.c.s. for $\{A_n\}$ with $\{B_{n,t}\} \sim_\lambda (f_t, D_t)$, i.e.,*

$$\lim_{n \rightarrow \infty} \sum_{j=1}^{d_n} \frac{F(\lambda_j(B_{n,t}))}{d_n} = \frac{1}{\mu(D_t)} \int_{D_t} \sum_{k=1}^p \frac{F(\lambda_k(f_t(s)))}{p} ds = \alpha_t(F)$$

for every $F \in C_c(\mathbb{R})$. Assume that, for every $F \in C_c(\mathbb{R})$,

$$\lim_{t \rightarrow \infty} \alpha_t(F) = \alpha(F).$$

Then

$$\lim_{n \rightarrow \infty} \sum_{j=1}^{d_n} \frac{F(\lambda_j(A_n))}{d_n} = \alpha(F). \quad (6)$$

If in addition we have

$$\lim_{t \rightarrow \infty} f_t^E = f \quad (7)$$

in D almost everywhere, with

$$f_t^E = \begin{cases} f_t(s) & \text{if } s \in D_t \\ 0 & \text{otherwise,} \end{cases}$$

then we write $\{A_n\} \sim_{\lambda, \text{moving}}(f, D)$. Moreover, if $\mu(D) < \infty$, we have

$$\alpha(F) = \frac{1}{\mu(D)} \int_D \sum_{k=1}^p \frac{F(\lambda_k(f(s)))}{p} ds.$$

4.1 Generalized Approximating class of sequences

In this section, we introduce a new tool inspired by the a.c.s. theory and by the extradimensional approach (see [29], Section 4.1 and Section 4.2), but more flexible and able to handle all the parameters needed in order to study discretizations on unbounded domains of finite measure, or moving domains. As for the classical a.c.s. tool, also the notion of generalized a.c.s. carries information about spectral and singular value distribution, which is what we prove in Theorem 4.3. Hereafter, we focus on domains with finite measure, which will be the ones treated in the numerical tests.

Definition 4.1. Let $\{A_n\}_n$ be a matrix-sequence of size $d_n \times d'_n$ with d_n and d'_n monotonically increasing integer sequences and let $\{\{B_{n,t}\}_n\}_t$ be a sequence of matrix-sequences of size $d_{n,t} \times d'_{n,t}$. We say that $\{\{B_{n,t}\}_n\}_t$ is a generalized approximating class of sequences (g.a.c.s.) for $\{A_n\}_n$ if, for every t , there exists n_t such that, for $n > n_t$,

$$A_n = U_{n,t} (B_{n,t} \oplus 0_{n,t}) V_{n,t} + R_{n,t} + N_{n,t},$$

where $0_{n,t}$ is the null matrix of size $(d_n - d_{n,t}) \times (d'_n - d'_{n,t})$, $U_{n,t}$ and $V_{n,t}$ are two unitary matrices of order $d_n \times d_n$ and $d'_n \times d'_n$ respectively and $R_{n,t}, N_{n,t}$ are matrices of the same size of A_n , satisfying:

$$\text{rank}(R_{n,t}) \leq c(t) d_n \wedge d'_n,$$

$$\|N_{n,t}\| \leq \omega(t),$$

$$d_n \wedge d'_n - d_{n,t} \wedge d'_{n,t} =: m_{n,t} \leq m(t) d_n \wedge d'_n,$$

$$\lim_{t \rightarrow \infty} c(t) = \lim_{t \rightarrow \infty} \omega(t) = \lim_{t \rightarrow \infty} m(t) = 0.$$

If we have a sequence $\{A_n\}_n$ of square Hermitian matrices, we also ask $\{\{B_{n,t}\}_n\}_t$ to be square Hermitian and $V_{n,t} = U_{n,t}^*$ for all n and t .

Remark 4.1. The notion of *g.a.c.s.* is intended as a generalization of the idea of *a.c.s.* being more natural when dealing with the approximation of infinite dimensional operators over moving or unbounded domains. In particular, in the case of a discretization of a (fractional) differential operator over moving or unbounded domains we usually end up with a sequence of domains (either a precompact exhaustion of the unbounded domain or the sequence of moving domains or a combination of both). Using the same approximation procedure (Finite Differences, Finite Elements, Isogeometric Analysis, Finite Volumes etc), it is natural to obtain matrices of different dimensions and *g.a.c.s.* is intended as a tool for dealing with this difficulty in the spirit of the extradimensional approach used in Sections 4.1, 4.2 in [29].

Theorem 4.3. Let $\{A_n\}$ be a matrix-sequence of size $d_n \times d'_n$ with d_n and d'_n monotonically increasing integer sequences. Let $\{\{B_{n,t}\}_n\}_t$ be a *g.a.c.s.* for $\{A_n\}$. If, $\forall t, \exists (f_t, D_t)$ such that:

- $\{\{B_{n,t}\}_n\}_t \sim_\sigma (f_t, D_t)$,
- $D_t \subset D_{t+1}, \forall t$,
- $D := \bigcup_{t>0} D_t$ of finite measure,
- $\exists f : D \rightarrow \mathbb{C}^{p_1 \times p_2}, p_1, p_2 \geq 1$, measurable such that $f_t^E \rightarrow f$ in measure, $t \rightarrow +\infty$, with $p = p_1 \wedge p_2$ and

$$f_t^E = \begin{cases} f_t(s) & \text{if } s \in D_t \\ 0 & \text{if } s \in D \setminus D_t, \end{cases}$$

then $\{A_n\} \sim_\sigma (f, D)$, i.e.

$$\lim_{n \rightarrow \infty} \sum_{j=1}^{d_n \wedge d'_n} \frac{F(\sigma_j(A_n))}{d_n \wedge d'_n} = \frac{1}{\mu(D)} \int_D \sum_{k=1}^p \frac{F(\sigma_k(f(s)))}{p} ds, \quad \forall F \in C_c(\mathbb{R}) \quad (8)$$

Proof. First, we note that relation (8) is true if and only if it is true for any F in C^1 with bounded support by simple functional approximation techniques. At this point, taking $F = F^\uparrow + F^\downarrow$, with $F^\uparrow(x) = \int_{-\infty}^x (F')^+(t) dt$ and $F^\downarrow(x) = \int_{-\infty}^x (F')^-(t) dt$, where $g^+ = \max(g, 0)$ and $g^- = \max(-g, 0)$, we deduce by linearity that (8) is true if and only if it holds for every G continuous, differentiable (with G' nonnegative), being equal to 0 for every $x \leq c_1$ and being constant (equal to $\|G\|_\infty$) for every $x \geq c_2$.

Since, by hypothesis, $\{\{B_{n,t}\}_n\}_t \sim_\sigma (f_t, D_t)$, $D_t \subset D_{t+1}$ and $D := \bigcup_{t>0} D_t$ is of finite measure, we have:

$$0 < \mu(D_t) \leq \mu(D_{t+1}) \rightarrow \mu(D) < +\infty, \quad t \rightarrow +\infty$$

and, since $f_t^E \rightarrow f$ in measure, $t \rightarrow +\infty$, we also have

$$\sigma_k(f_t^E) \rightarrow \sigma_k(f) \quad \text{in measure} \quad \forall 1 \leq k \leq p$$

hence,

$$\begin{aligned} \lim_{t \rightarrow \infty} \frac{1}{\mu(D_t)} \int_{D_t} \sum_{k=1}^p \frac{G(\sigma_k(f_t(s)))}{p} ds &= \lim_{t \rightarrow \infty} \frac{\mu(D)}{\mu(D_t)} \frac{1}{\mu(D)} \left(\int_D \sum_{k=1}^p \frac{G(\sigma_k(f_t^E(s)))}{p} ds - G(0)\mu(D \setminus D_t) \right) = \\ &= \frac{1}{\mu(D)} \int_D \sum_{k=1}^p \frac{G(\sigma_k(f(s)))}{p} ds \end{aligned} \quad (9)$$

Now, since $\forall n > n_t$ $A_n = U_{n,t}(B_{n,t} \oplus 0_{n,t})V_{n,t} + R_{n,t} + N_{n,t}$, we set $C_{n,t} = U_{n,t}(B_{n,t} \oplus 0_{n,t})V_{n,t}$ and we notice that the singular values of $C_{n,t}$ are the singular values of $B_{n,t}$ with $m_{n,t} = d_n \wedge d'_n - d_{n,t} \wedge d'_{n,t}$ additional singular values equal to zero. By classic results of interlacing of singular values under rank and norm corrections, we have

$$\sigma_j(A_n) = \sigma_j(C_{n,t} + R_{n,t} + N_{n,t}) \leq \sigma_j(C_{n,t} + R_{n,t}) + \omega(t) \leq \sigma_{j+(d_n \wedge d'_n)c(t)}(C_{n,t}) + \omega(t)$$

where $\sigma_j(C_{n,t}) := +\infty$ for $j > d_n \wedge d'_n$. On the basis of the initial discussion, we take G differentiable, monotone non-decreasing, positive and bounded (so $\|G\|_\infty = G(+\infty)$) and we have:

$$\begin{aligned} \sum_{j=1}^{d_n \wedge d'_n} \frac{G(\sigma_j(A_n))}{d_n \wedge d'_n} &= \sum_{j=1}^{d_n \wedge d'_n} \frac{G(\sigma_j(C_{n,t} + R_{n,t} + N_{n,t}))}{d_n \wedge d'_n} \leq \\ &\leq \sum_{j=1}^{d_n \wedge d'_n} \frac{G(\sigma_{j+(d_n \wedge d'_n)c(t)}(C_{n,t}) + \omega(t))}{d_n \wedge d'_n} \leq \sum_{j=1}^{d_n \wedge d'_n} \frac{G(\sigma_{j+(d_n \wedge d'_n)c(t)}(C_{n,t}))}{d_n \wedge d'_n} + \omega(t) \|G'\|_\infty \leq \\ &\leq \sum_{j=1+(d_n \wedge d'_n)c(t)}^{d_n \wedge d'_n} \frac{G(\sigma_j(C_{n,t}))}{d_n \wedge d'_n} + c(t) \|G\|_\infty + \omega(t) \|G'\|_\infty \leq \sum_{j=1}^{d_n \wedge d'_n} \frac{G(\sigma_j(C_{n,t}))}{d_n \wedge d'_n} + c(t) \|G\|_\infty + \omega(t) \|G'\|_\infty \end{aligned} \quad (10)$$

Taking into account the information about the singular values of $C_{n,t}$, it follows that:

$$\begin{aligned} \sum_{j=1}^{d_n \wedge d'_n} \frac{G(\sigma_j(C_{n,t}))}{d_n \wedge d'_n} &= \frac{d_{n,t} \wedge d'_{n,t}}{d_n \wedge d'_n} \sum_{j=1}^{d_{n,t} \wedge d'_{n,t}} \frac{G(\sigma_j(B_{n,t}))}{d_{n,t} \wedge d'_{n,t}} + \frac{m_{n,t}}{d_n \wedge d'_n} G(0) \leq \\ &\leq \sum_{j=1}^{d_{n,t} \wedge d'_{n,t}} \frac{G(\sigma_j(B_{n,t}))}{d_{n,t} \wedge d'_{n,t}} + m(t) \|G\|_\infty \end{aligned} \quad (11)$$

Now, given $\epsilon > 0$, we choose t large enough such that $\omega(t), c(t), m(t) < \epsilon$ and also, by (9):

$$\frac{1}{\mu(D_t)} \int_{D_t} \sum_{k=1}^p \frac{G(\sigma_k(f_t(s)))}{p} ds \leq \frac{1}{\mu(D)} \int_D \sum_{k=1}^p \frac{G(\sigma_k(f(s)))}{p} ds + \epsilon \quad (12)$$

Once t is fixed, using that $\{\{B_{n,t}\}_n\}_t \sim_\sigma (f_t, D_t)$, we can find $N_\epsilon > n_t$ such that $\forall n > N_\epsilon$ we have:

$$\sum_{j=1}^{d_{n,t} \wedge d'_{n,t}} \frac{G(\sigma_j(B_{n,t}))}{d_{n,t} \wedge d'_{n,t}} \leq \frac{1}{\mu(D_t)} \int_{D_t} \sum_{k=1}^p \frac{G(\sigma_k(f_t(s)))}{p} ds + \epsilon \quad (13)$$

Finally, using the derivations in (10),(11),(12) and (13), $\forall n > N_\epsilon$ we get:

$$\begin{aligned} \sum_{j=1}^{d_n \wedge d'_n} \frac{G(\sigma_j(A_n))}{d_n \wedge d'_n} &\leq \sum_{j=1}^{d_n \wedge d'_n} \frac{G(\sigma_j(C_{n,t}))}{d_n \wedge d'_n} + c(t) \|G\|_\infty + \omega(t) \|G'\|_\infty \leq \\ &\leq \sum_{j=1}^{d_{n,t} \wedge d'_{n,t}} \frac{G(\sigma_j(B_{n,t}))}{d_{n,t} \wedge d'_{n,t}} + (m(t) + c(t)) \|G\|_\infty + \omega(t) \|G'\|_\infty \leq \end{aligned}$$

$$\begin{aligned}
&\leq \frac{1}{\mu(D_t)} \int_{D_t} \sum_{k=1}^p \frac{G(\sigma_k(f_t(s)))}{p} ds + (1 + 2\|G\|_\infty + \|G'\|_\infty)\epsilon \leq \\
&\leq \frac{1}{\mu(D)} \int_D \sum_{k=1}^p \frac{G(\sigma_k(f(s)))}{p} ds + (2 + 2\|G\|_\infty + \|G'\|_\infty)\epsilon
\end{aligned}$$

Since ϵ is arbitrary, we get

$$\limsup_{n \rightarrow \infty} \sum_{j=1}^{d_n \wedge d'_n} \frac{G(\sigma_j(A_n))}{d_n \wedge d'_n} \leq \frac{1}{\mu(D)} \int_D \sum_{k=1}^p \frac{G(\sigma_k(f(s)))}{p} ds$$

In a similar we can obtain also that

$$\liminf_{n \rightarrow \infty} \sum_{j=1}^{d_n \wedge d'_n} \frac{G(\sigma_j(A_n))}{d_n \wedge d'_n} \geq \frac{1}{\mu(D)} \int_D \sum_{k=1}^p \frac{G(\sigma_k(f(s)))}{p} ds$$

we just need to be a bit more careful in two of the passages, when, using that G is positive, we added terms in the sum in (10) and used that $d_{n,t} \wedge d'_{n,t} \leq d_n \wedge d'_n$ in (11). Nevertheless, those two additional terms of correction depend on G , $c(t)$ and $m(t)$ and can be controlled similarly to those coming from limsup derivations. This ends the proof. \square

Under the hypothesis that the sequences are Hermitian, we can extend the previous result to the case of eigenvalues (with essentially the same proof), getting the following theorem.

Theorem 4.4. *Let $\{A_n\}$ be a sequence of Hermitian matrices of size d_n with d_n a monotonically increasing integer sequence. Let $\{\{B_{n,t}\}_n\}_t$ be a g.a.c.s. for $\{A_n\}$ (in the Hermitian sense). If, $\forall t, \exists (f_t, D_t)$ such that:*

- $\{\{B_{n,t}\}_n\}_t \sim_\lambda (f_t, D_t)$,
- $D_t \subset D_{t+1}, \forall t$,
- $D := \bigcup_{t>0} D_t$ of finite measure,
- $\exists f : D \rightarrow \mathbb{C}^{p \times p}$ measurable such that $f_t^E \rightarrow f$ in measure, $t \rightarrow +\infty$, with

$$f_t^E = \begin{cases} f_t(s) & \text{if } s \in D_t \\ 0 & \text{if } s \in D \setminus D_t, \end{cases}$$

then $\{A_n\} \sim_\lambda (f, D)$.

Remark 4.2. *In the case of domains of infinite measure we expect that a similar extension as the one obtained for a.c.s. can be obtained. We do not go into detail at the moment as we want to focus mainly on unbounded domains with finite measure, leaving this possible extension for future developments. At any rate, as Theorem 4.1 and Theorem 4.2 show, the infinite measure setting can be handled: however, we still need to make a fine tuning of the new concepts in order to work in the best possible way.*

5 Applications, examples, numerical evidences

In this section we show a few basic numerical examples for proving the validity of the theory developed in the previous section. We start with a kind of trivial one in a bounded setting and then explore a more involved one where the domain is unbounded with finite measure and hence, of course, of non-Cartesian type: in this case we consider both P_1 and P_2 Finite Elements and as operator both the constant coefficient and the variable coefficient Laplacian.

5.1 Approximating by Finite Elements over an exhaustion of $(0,1)$

We consider the following model problem

$$\begin{cases} -\Delta u = f & \text{on } (0,1) \\ u(0) = u(1) = 0. \end{cases}$$

It is probably the most studied test example and it is already known that its P_1 Finite Elements approximation [8] on a uniform grid with a proper scaling leads to the solution of a linear system whose coefficient matrix is $A_n = T_n(2 - 2 \cos(\theta))$. As widely known related sequence $\{A_n\}_n$ has a spectral distribution given by the function $2 - 2 \cos(\theta)$ in $[-\pi, \pi]$: it is indeed a special case of Theorem 3.1 since its symbol is real-valued. We can see this also by applying linear Finite Elements to the problem

$$\begin{cases} -\Delta u = f & \text{on } (0, 1 - 1/t) \\ u(0) = u(1 - 1/t) = 0. \end{cases}$$

In this case the spectral distribution of the associated matrix sequence $\{B_{n,t}\}$ is given by the symbol function $(1 - 1/t)(2 - 2 \cos(\theta))$ for every $t > 0$. Clearly, all the assumption of Theorem 4.2 are satisfied, hence the sequence $\{A_n\}_n$ has spectral distribution with symbol given by $\lim_{t \rightarrow \infty} (1 - 1/t)(2 - 2 \cos(\theta)) = 2 - 2 \cos(\theta)$.

Remark 5.1. *We note that one of the main aspects that allows us to infer the spectral distribution of the sequence $\{A_n\}_n$ is the “convergence” of the points in the discretization defining $\{\{B_{n,t}\}\}$ (and of the related domain) to those defining $\{A_n\}$ (and of the limit domain) as $t \rightarrow \infty$. In fact, this is what makes $\{\{B_{n,t}\}\}$ an a.c.s. for $\{A_n\}$.*

5.2 Quadratic Finite Elements for the model problem on a two-dimensional unbounded set of finite measure

We consider the following problem

$$\begin{cases} -\Delta u = v & \text{on } \Omega \\ u = 0 & \text{on } \partial\Omega, \end{cases} \quad (14)$$

where $\Omega = \{(x, y) \in \mathbb{R}^2 : x > 0, y > 0 \text{ and } y < g(x)\}$ with

$$g(x) = \begin{cases} 1 & x < 1 \\ \frac{1}{x^2} & x \geq 1. \end{cases}$$

It is clear that $\mu(\Omega) = \int_0^\infty g(x)dx = 2 < \infty$. For the discretization, we consider as space-step $h = \frac{1}{n+1}$ and the nodes $(x_i, y_j) = (ih, jh)$. We consider the maximum value of i, \bar{i} , for which there exists j such that $(x_{\bar{i}}, y_j) \in \Omega$. We consider all the points in the rectangle $(0, \bar{i}) \times (0, 1)$. Note that the index $\bar{i} = \lfloor \sqrt{n+1} \rfloor$.

On these points we apply quadratic P_2 Finite Elements which leads to a two-level Toeplitz matrix $T_{\mathbf{n}}(f)$ with $\mathbf{n} = (n, n \lfloor \sqrt{n+1} \rfloor)$ and $f = f_{P_2} : [-\pi, \pi]^2 \rightarrow \mathbb{C}^{4 \times 4}$ (see [34]) with

$$f = f_{P_2}(\theta_1, \theta_2) = \left[\begin{array}{cc|cc} \alpha & -\beta(1 + e^{i\theta_1}) & -\beta(1 + e^{i\theta_2}) & 0 \\ -\beta(1 + e^{-i\theta_1}) & \alpha & 0 & -\beta(1 + e^{i\theta_2}) \\ \hline -\beta(1 + e^{-i\theta_2}) & 0 & \alpha & -\beta(1 + e^{i\theta_1}) \\ 0 & -\beta(1 + e^{-i\theta_2}) & -\beta(1 + e^{-i\theta_1}) & \gamma + \frac{\beta}{2}(\cos(\theta_1) + \cos(\theta_2)) \end{array} \right] \quad (15)$$

where $\alpha = 16/3$, $\beta = 4/3$, and $\gamma = 4$.

Clearly, this sequence has spectral distribution given by f on the domain $[-\pi, \pi]^2$ by Theorem 3.1 since its symbol is Hermitian-valued: indeed given the even nature of the symbol the domain can be reduce to the subdomain $[0, \pi]^2$. We now consider the points $(x_i, y_j) \in \Omega$ and the points $(x_i, y_j) \in \Omega_t = \Omega \cap B(0, t)^{\|\cdot\|_\infty}$. As $h \rightarrow 0$ we obtain uniform discretizations both for the set Ω and for the sets Ω_t , which constitute an exhaustion of the domain Ω . Finally, we can obtain a discrete version $A_{\mathbf{n}}$ of the Laplacian on Ω by simply cutting from the matrix $T_{\mathbf{n}}(f)$ all the rows and columns corresponding to indices (i, j) such that (x_i, y_j) are not in Ω . We can do the same on Ω_t obtaining another sequence of matrices $\{C_{\mathbf{n},t}\}$. In general $\dim(A_{\mathbf{n}}) \neq \dim(C_{\mathbf{n},t})$. We then consider the sequence $\{B_{\mathbf{n},t}\}$, where $B_{\mathbf{n},t} = C_{\mathbf{n},t} \oplus 0_m$ and m is such that $\dim(B_{\mathbf{n},t}) = \dim(A_{\mathbf{n}})$. We want to prove that

- a) there exists f_t such that $\{B_{\mathbf{n},t}\} \sim_{\lambda, \sigma} (f_t, \Omega \times [-\pi, \pi]^2)$.
- b) $\{B_{\mathbf{n},t}\}$ is an a.c.s. for a matrix-sequence $\{\tilde{A}_{\mathbf{n}}\}$ where $\tilde{A}_{\mathbf{n}}$ is similar to $A_{\mathbf{n}}$ for every \mathbf{n} using a unique permutation matrix.
- c) $\exists \lim_{t \rightarrow \infty} f_t$ in $\Omega \times [-\pi, \pi]^2$.

Using Theorem 4.1 and Theorem 4.2, we can conclude that $\{A_{\mathbf{n}}\} \sim_{\lambda, \sigma} (f, \Omega \times [-\pi, \pi]^2)$.

For item a) we can simply use the theory of reduced GLT in [2], obtaining that $\{B_{\mathbf{n},t}\} \sim_{\lambda, \sigma} (f_t, \Omega \times [-\pi, \pi]^2)$, with $f_t(\mathbf{x}, \theta_1, \theta_2) = \chi_{\Omega_t}(\mathbf{x}) \cdot f$, with f depending on the used approximation of the considered PDE and $\mathbf{x} = (x, y)$.

For item b) we note that $\tilde{A}_{\mathbf{n}} = B_{\mathbf{n},t} + R_{\mathbf{n},t}$ with $\text{rank}(R_{\mathbf{n},t}) \leq (2 - \mu(\Omega_t))n^2 + c(t)n$, where $c(t) \rightarrow 0$ as $t \rightarrow \infty$. Since $\mu(\Omega_t) \rightarrow 2$ as $t \rightarrow \infty$, we find that $\{B_{\mathbf{n},t}\}$ is an a.c.s. for $\{\tilde{A}_{\mathbf{n}}\}$.

For item c) we have

$$\lim_{t \rightarrow \infty} f_t = f$$

for every $(\mathbf{x}, \theta_1, \theta_2) \in \Omega \times [-\pi, \pi]^2$. Using Theorem 4.1 and Theorem 4.2, recalling Definition 2.1, we conclude that the sequence $\{A_{\mathbf{n}}\}$ has a distribution both in the eigenvalue sense and in the spectral value sense given by f on $\Omega \times [-\pi, \pi]^2$ or equivalently on $\Omega \times [0, \pi]^2$.

Remark 5.2. *Equivalently, we can choose as $B_{\mathbf{n},t}$ the matrix defined by $D_{\mathbf{n}}(\chi_{\Omega_t})A_{\mathbf{n}}D_{\mathbf{n}}(\chi_{\Omega_t})$ and it is possible to see that the rank of $A_{\mathbf{n}} - B_{\mathbf{n},t}$ satisfies the same upper estimate as above and $\{B_{\mathbf{n},t}\}$ is still distributed as $(f_t, \Omega \times [-\pi, \pi]^2)$. Furthermore the set $[-\pi, \pi]^2$ can be replaced by $[0, \pi]^2$ in all cases in which the function is even in θ_1, θ_2 , separately. As already observed in [41][pp. 375-378], it is worth recalling that the obtained spectral symbol depends on three actors: the operator order, the coefficients/physical domain, the approximation technique. For instance in our setting the underlying operator has order two and this can be read in the minimal eigenvalue of the symbol which is asymptotic to $2 - 2 \cos(\theta)$ in one variable and to $4 - 2 \cos(\theta_1) - 2 \cos(\theta_2)$ in two variables. In both cases the order of the zero is two and this decides the conditioning of the resulting matrices which will grow as $N^{\frac{2}{d}}$ with N being the matrix-size and d the dimensionality of the domain Ω . However, there are also other features that can be recovered. Here we mention three of them:*

- the fact that the zero is at zero informs that the subspace related to low frequencies is the one associated with the small eigenvalues,
- an unbounded diffusion coefficient $a(x, y)$ e.g. with a unique pole at (\hat{x}, \hat{y}) of order γ will be seen in the maximal eigenvalues exploding as $N^{\frac{\gamma}{d}}$ and the related subspaces that can be easily identified as a function of the point (\hat{x}, \hat{y}) : in this case the overall conditioning will be asymptotic to $N^{\frac{(2+\gamma)}{d}}$.
- The approximation technique plays a role in the structure on the underlying matrices and hence in the complexity of the associated matrix-vector product: the more the method is precise the larger is the bandwidth in a multilevel sense, while the number of levels is decided by the dimensionality of the physical domain Ω , and the presence of blocks and their size is exactly the gap between the degree of the polynomials used in the Finite Elements and the global continuity which is imposed (see also the discussion at the end of the introduction).

The remark below concerns the approximation by Q_2 Finite Elements, i.e., using rectangles as basic geometric elements instead of triangles. Notice that the curve $y = \frac{1}{x^2}$ for $x \geq 1$ defining the domain is better approximated using triangles instead of rectangles that would give an unpleasant staircase.

Remark 5.3. Consider the quadratic Finite Elements approximation of the considered one-dimensional model problem. The resulting stiffness matrix is essentially of block Toeplitz type with blocks

$$K_0 = \frac{1}{3} \begin{bmatrix} 16 & -8 \\ -8 & 14 \end{bmatrix}, \quad K_1 = \frac{1}{3} \begin{bmatrix} 0 & -8 \\ 0 & 1 \end{bmatrix}.$$

Similarly, according to [22], the corresponding blocks of the mass matrix are

$$M_0 = \frac{1}{15} \begin{bmatrix} 8 & 1 \\ 1 & 4 \end{bmatrix}, \quad M_1 = \frac{1}{30} \begin{bmatrix} 0 & 2 \\ 0 & -1 \end{bmatrix}.$$

Furthermore, the symbol of the sequence of the stiffness matrices is the function

$$\mathbf{f}_2(\theta) = \frac{1}{3} \begin{bmatrix} 16 & -8 - 8e^{i\theta} \\ -8 - 8e^{-i\theta} & 14 + 2 \cos \theta \end{bmatrix}, \quad \theta \in [-\pi, \pi],$$

while the symbol of the sequence of the mass matrices is the function

$$\mathbf{h}_2(\theta) = \frac{1}{15} \begin{bmatrix} 8 & 1 + e^{i\theta} \\ 1 + e^{-i\theta} & 4 - \cos \theta \end{bmatrix}, \quad \theta \in [-\pi, \pi],$$

again in accordance to [22]. The eigenvalues of $\mathbf{f}_2(\theta)$, are

$$\begin{aligned} \lambda_1(\mathbf{f}_2(\theta)) &= 5 + \frac{1}{3} \cos \theta + \frac{1}{3} \sqrt{129 + 126 \cos \theta + \cos^2 \theta}, \\ \lambda_2(\mathbf{f}_2(\theta)) &= 5 + \frac{1}{3} \cos \theta - \frac{1}{3} \sqrt{129 + 126 \cos \theta + \cos^2 \theta} = \frac{16}{3} \frac{2 - 2 \cos \theta}{\lambda_1(\mathbf{f}_2(\theta))}. \end{aligned}$$

Similarly, the eigenvalues of $\mathbf{h}_2(\theta)$ are

$$\begin{aligned} \lambda_1(\mathbf{h}_2(\theta)) &= \frac{2}{5} - \frac{1}{30} \cos \theta + \frac{1}{30} \sqrt{24 + 16 \cos \theta + \cos^2 \theta}, \\ \lambda_2(\mathbf{h}_2(\theta)) &= \frac{2}{5} - \frac{1}{30} \cos \theta - \frac{1}{30} \sqrt{24 + 16 \cos \theta + \cos^2 \theta}. \end{aligned}$$

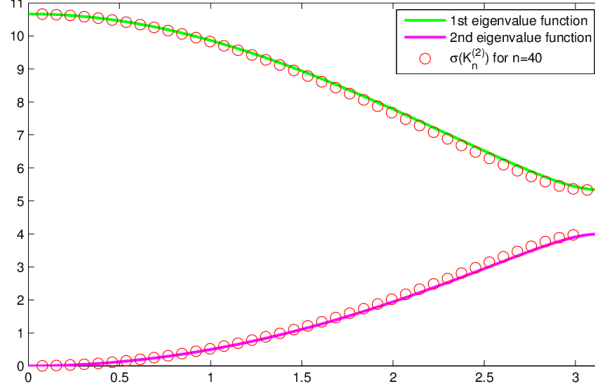


Figure 1: Graph over $[0, \pi]$ of the eigenvalue functions $\lambda_i(\mathbf{f}_2(\theta))$, $i = 1, 2$, and of the pairs $\left(\frac{k\pi}{n+1}, \lambda_k(K_n^{(2)})\right)$, $k = 1, \dots, n$, and $\left(\frac{(2n-k)\pi}{n+1}, \lambda_k(K_n^{(2)})\right)$, $k = n+1, \dots, 2n-1$, for $n = 40$.

Since the eigenvalue functions $\lambda_i(\mathbf{f}_2(\theta))$, $i = 1, 2$, are even, it follows from Definition 2.1 that $\mathbf{f}_2(\theta)$ restricted to $[0, \pi]$ is still a symbol for $\{K_n^{(2)}\}_n$. As already recalled in the Introduction, the latter is equivalent to write that a suitable ordering of the eigenvalues $\lambda_j(K_n^{(2)})$, $j = 1, \dots, 2n-1$, assigned in correspondence with an equispaced grid on $[0, \pi]$, reconstructs approximately the graphs of the eigenvalue functions $\lambda_i(\mathbf{f}_2(\theta))$, $i = 1, 2$. Setting $K_n^{(2)}$ the stiffness matrix in one dimension, this is observed in Figure 1, where we fixed the equispaced grid $\frac{k\pi}{n+1}$, $k = 1, \dots, n$, in $[0, \pi]$ and we plotted the eigenvalue functions $\lambda_i(\mathbf{f}_2(\theta))$, $i = 1, 2$, as well as the pairs $\left(\frac{k\pi}{n+1}, \lambda_k(K_n^{(2)})\right)$, $k = 1, \dots, n$, and $\left(\frac{(2n-k)\pi}{n+1}, \lambda_k(K_n^{(2)})\right)$, $k = n+1, \dots, 2n-1$, for $n = 40$. We clearly see from Figure 1 that the eigenvalues of $K_n^{(2)}$ can be split into two subsets (or branches) of approximately the same cardinality; and the i -th branch is approximately given by a uniform sampling over $[0, \pi]$ of the i -th eigenvalue function $\lambda_i(\mathbf{f}_2(\theta))$, $i = 1, 2$.

The spectral symbol in the two-dimensional case is then

$$f = f_{Q_2}(\theta_1, \theta_2) = \mathbf{f}_2(\theta_1)\mathbf{h}_2(\theta_2) + \mathbf{h}_2(\theta_1)\mathbf{f}_2(\theta_2)$$

according to formula (5.1) in [22] and with $\mathbf{f}_2, \mathbf{h}_2$ as before. Interestingly enough the dimensionality of the two symbols f_{P_2}, f_{Q_2} is the same: two variables and matrix-size equal to four. Furthermore in both cases three eigenvalues are strictly positive and only one of them is asymptotic to the symbol of the standard discrete Laplacian by Finite Differences or P_1 Finite Elements, i.e., $4 - 2\cos(\theta_1) - 2\cos(\theta_2)$: compare [34] and [22].

Indeed, in the case of a general PDE with variable coefficients in a d -dimensional domains with standard Finite Elements the number of variables is $2d$ which reduces to d if the coefficients of the differential operator are constants and the dimensionality is k^d where k is the degree of the used polynomials in the Finite Elements. For diminishing the presence of an exponential number of branches, as discussed in the introduction, the solution is the Isogeometric analysis [23].

Finally we consider a variable coefficient version of the previous PDE in (14) expressed as follows

$$\begin{cases} \operatorname{div}(-a\nabla u) = v & \text{on } \Omega \\ u = 0 & \text{on } \partial\Omega, \end{cases} \quad (16)$$

where $a(x, y)$ is a positive non-degenerate variable coefficient on $\Omega = \{(x, y) \in \mathbb{R}^2 : x > 0, y > 0 \text{ and } y <$

$g(x)$ with

$$g(x) = \begin{cases} 1 & x < 1 \\ \frac{1}{x^2} & x \geq 1. \end{cases}$$

Notice that for $a \equiv 1$ problem (16) reduces to (14). As in the constant coefficient case we opt for basic P_1 Finite Elements. According to the theory reported in [22, 34] the symbol is

$$f(\theta_1, \theta_2, x, y) = (4 - 2 \cos \theta_1 - 2 \cos \theta_2) a(x, y),$$

with four variables, (x, y) in the physical domain, (θ_1, θ_2) in the Fourier domain, and dimensionality 1 since the degree of the polynomials used in the finite element is 1.

5.3 Numerical evidences

In this subsection we show numerical tests and visualizations corroborating the analysis conducted in the previous subsection. We focus on essentially few discretization techniques for the approximation of (14) and (16), namely standard centered Finite Differences of order two, P_1 Finite Elements, Q_1 Finite Elements, and P_2 Finite Elements.

With reference to Remark 5.2, we observed that the conditioning of the resulting matrices grows as $N^{\frac{2}{d}}$ with N being the matrix-size and d being the dimensionality. This is due to the minimal eigenvalue which converges to zero as $N^{-\frac{2}{d}}$ (see [38, 39, 6] for the pure Toeplitz setting and [33, 49] for the variable coefficient case) and the related property can be seen in Figures 2, 18, 34 where the univariate unique nondecreasing rearrangement of the symbol for $d = 2$ has a positive bounded derivative so that the minimal eigenvalue tends to zero as N^{-1} . Things do not change, as expected, in the variable coefficient setting since the diffusion coefficient $a(x, y)$ is positive and bounded: see Figure 50. For the rest there is nothing much to comment given the very strong agreement of the spectral behavior of the global matrix-sequences and of the corresponding approximations $\{\{B_{\mathbf{n},t}\}\}$, $\{\{C_{\mathbf{n},t}\}\}$ as t grows. The very striking fact is that the convergence is appreciated already for moderate values of t giving an evidence of the practical use of the used tools i.e. the notion of a.c.s and that, which is indeed more natural, of the generalized a.c.s.: for the details on the approximating matrices refer to the figures with even numbering from 4 to 16, from 20 to 32, from 36 to 48, from 52 to 64, and compare with Figures 2, 18, 34, 50 regarding the various matrix-sequences $\{A_{\mathbf{n}}\}$, respectively. Furthermore, in the figures with odd numbering from 3 to 65, the errors in the eigenvalue predictions are reported: the pseudo-random behavior can be attributed to the non-decreasing (univariate) rearrangement of the spectral symbol of $\{A_{\mathbf{n}}\}$. When maintaining the complete number of variables a much smoother surface is expected. In addition, when looking at the figures related to the P_2 approximation we observe 4 points where the rearranged symbol is not differentiable and this corresponds to the 4 branches of the spectra since the symbol is 4×4 Hermitian-valued. Finally, when looking at the figures with even numbering from 50 to 64, we observe smoother curves and wider ranges and this is due to the variable coefficient $a(x, y)$, since any of the four eigenvalue functions in the constant coefficient case is multiplied by $a(x, y)$.

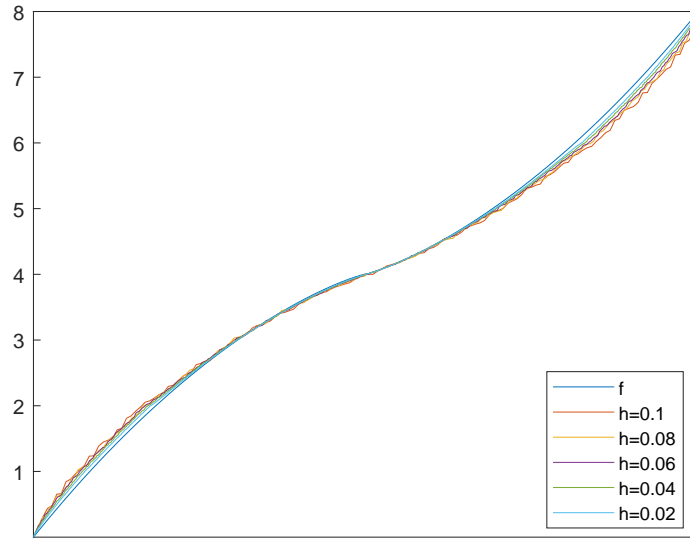


Figure 2: Eigenvalues distribution of A_n for different h values together with the sampling of $f(\theta_1, \theta_2) = (2 - 2 \cos \theta_1) + (2 - 2 \cos \theta_2)$.

5.3.1 Finite Differences/ P_1 - $f(\theta_1, \theta_2) = (2 - 2 \cos \theta_1) + (2 - 2 \cos \theta_2)$

Finite Differences/ P_1 : $f(\theta_1, \theta_2) = (2 - 2 \cos \theta_1) + (2 - 2 \cos \theta_2)$

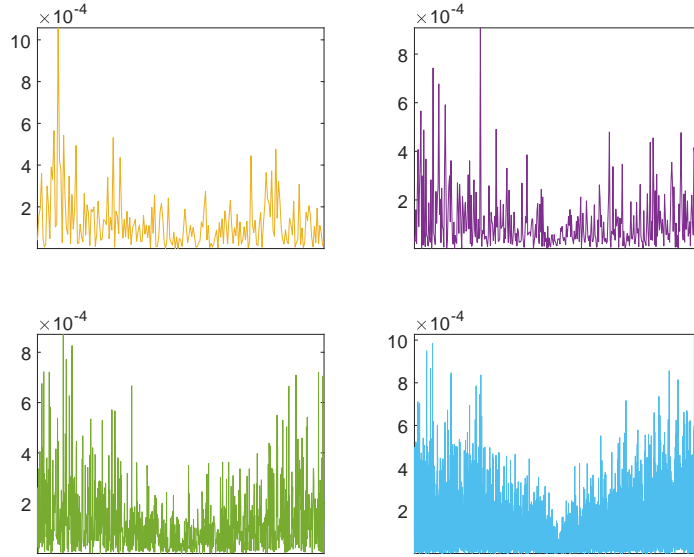


Figure 3: Minimal distance of eigenvalues of A_n from $f(\theta_1, \theta_2) = (2 - 2 \cos \theta_1) + (2 - 2 \cos \theta_2)$ for different h values.

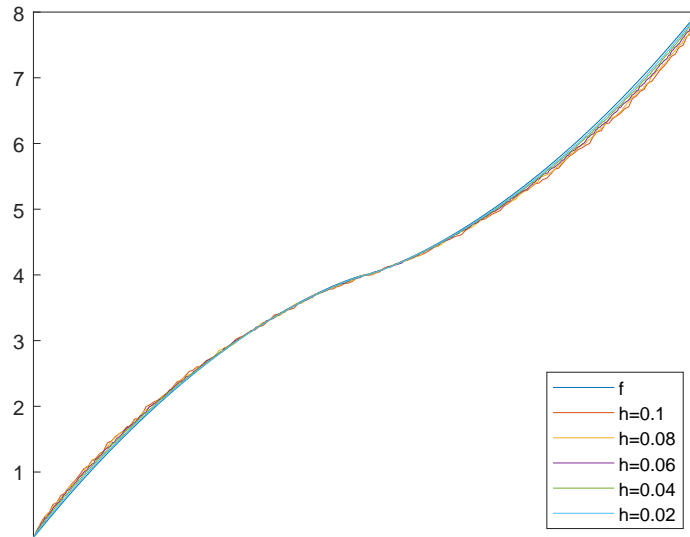


Figure 4: Eigenvalues distribution of $C_{n,t}$ for different h values together with the sampling of $f(\theta_1, \theta_2) = (2 - 2 \cos \theta_1) + (2 - 2 \cos \theta_2)$ and $t = 2$.

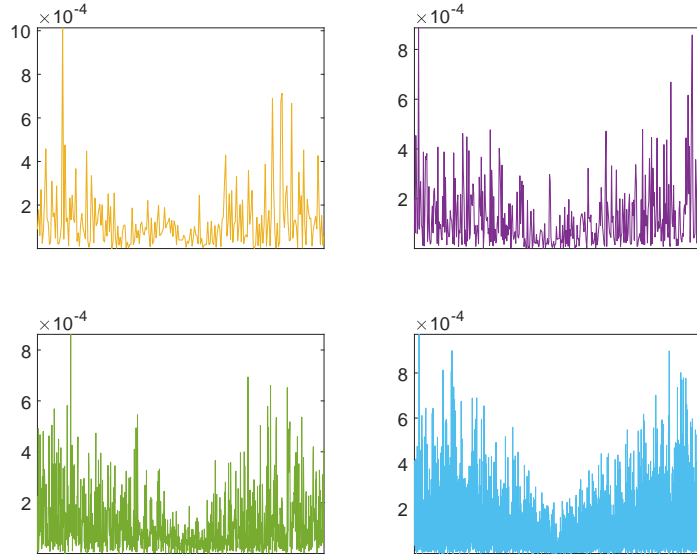


Figure 5: Minimal distance of eigenvalues of $C_{n,t}$ from $f(\theta_1, \theta_2) = (2 - 2 \cos \theta_1) + (2 - 2 \cos \theta_2)$ and $t = 2$ for different h values.

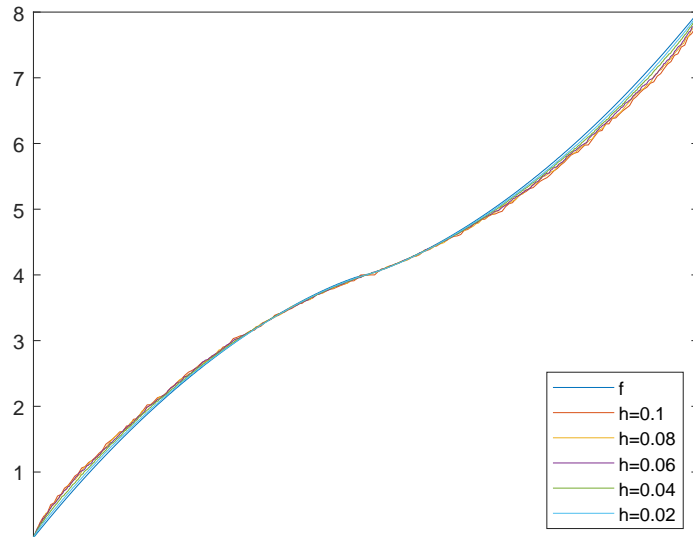


Figure 6: Eigenvalues distribution of $C_{n,t}$ for different h values together with the sampling of $f(\theta_1, \theta_2) = (2 - 2 \cos \theta_1) + (2 - 2 \cos \theta_2)$ and $t = 4$.

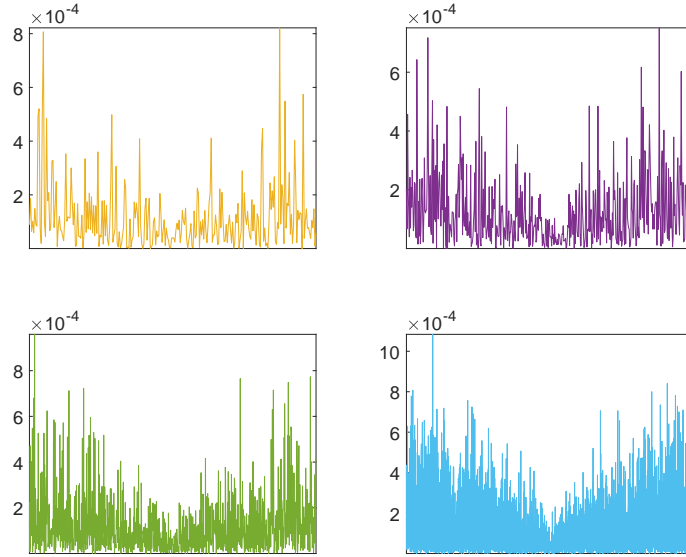


Figure 7: Minimal distance of eigenvalues of $C_{n,t}$ from $f(\theta_1, \theta_2) = (2 - 2 \cos \theta_1) + (2 - 2 \cos \theta_2)$ and $t = 4$ for different h values.

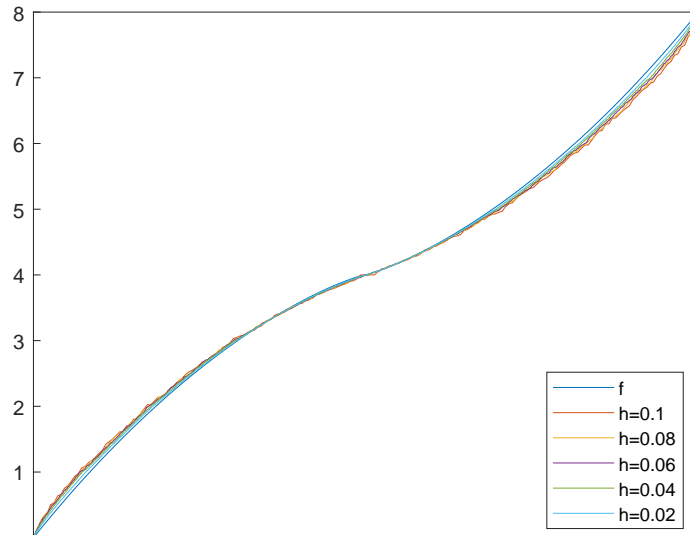


Figure 8: Eigenvalues distribution of $C_{n,t}$ for different h values together with the sampling of $f(\theta_1, \theta_2) = (2 - 2 \cos \theta_1) + (2 - 2 \cos \theta_2)$ and $t = 6$.

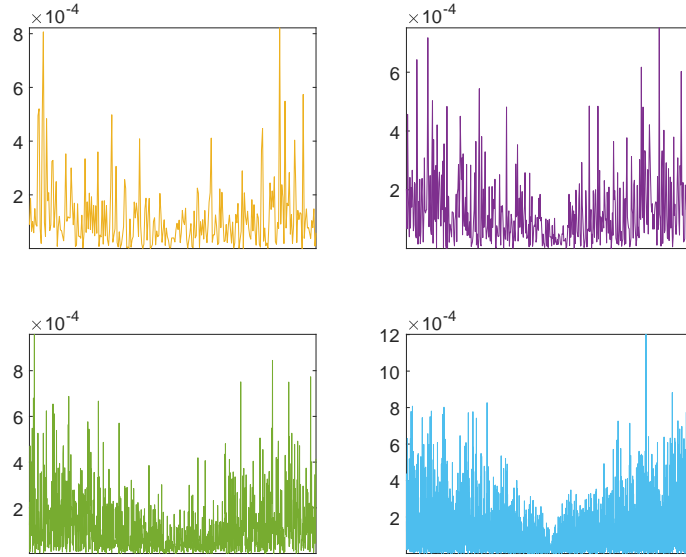


Figure 9: Minimal distance of eigenvalues of $C_{n,t}$ from $f(\theta_1, \theta_2) = (2 - 2 \cos \theta_1) + (2 - 2 \cos \theta_2)$ and $t = 6$ for different h values.

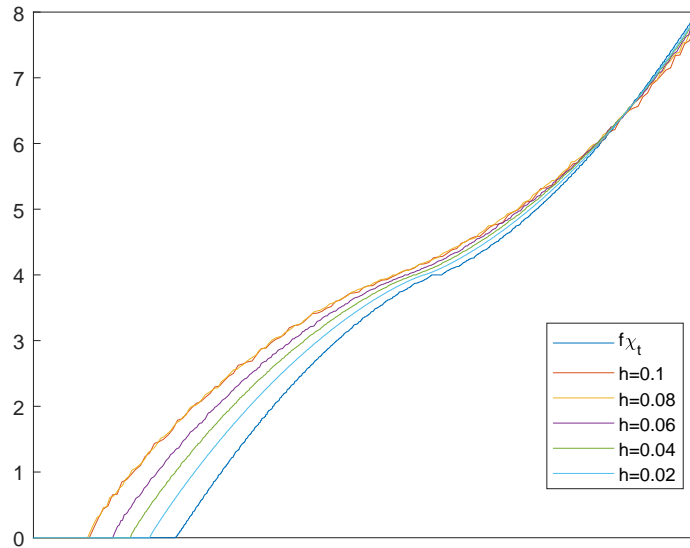


Figure 10: Eigenvalues distribution of $B_{n,t}$ for different h values together with the sampling of $f(\theta_1, \theta_2) = (2 - 2 \cos \theta_1) + (2 - 2 \cos \theta_2)$ and $t = 2$.

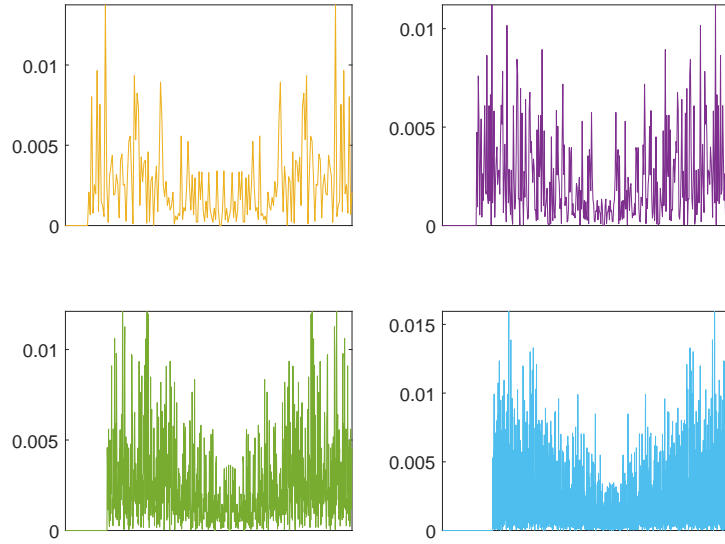


Figure 11: Minimal distance of eigenvalues of $B_{n,t}$ from $f(\theta_1, \theta_2) = (2 - 2 \cos \theta_1) + (2 - 2 \cos \theta_2)$ and $t = 2$ for different h values.

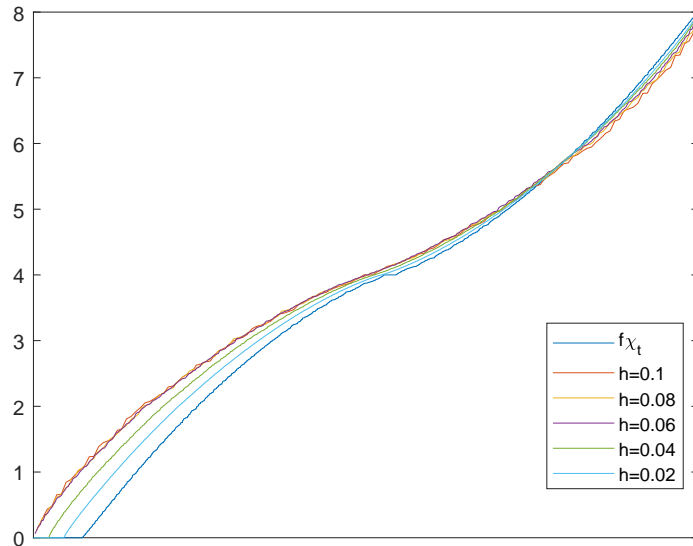


Figure 12: Eigenvalues distribution of $B_{n,t}$ for different h values together with the sampling of $f(\theta_1, \theta_2) = (2 - 2 \cos \theta_1) + (2 - 2 \cos \theta_2)$ and $t = 4$.

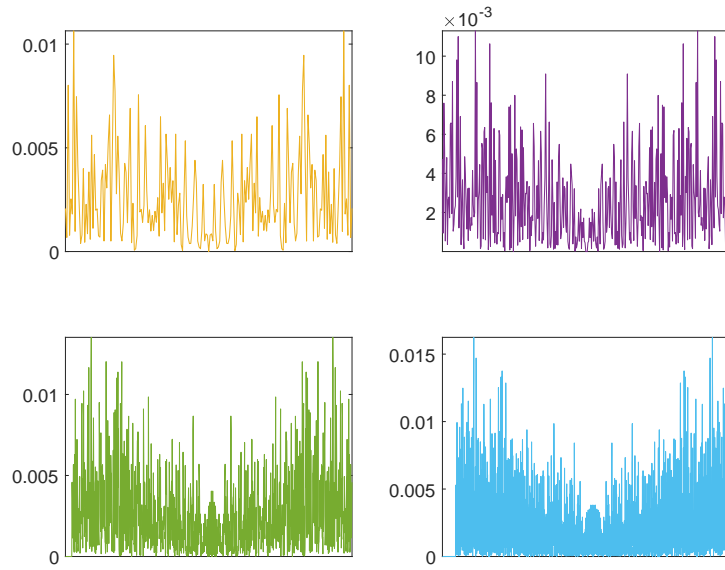


Figure 13: Minimal distance of eigenvalues of $B_{n,t}$ from $f(\theta_1, \theta_2) = (2 - 2 \cos \theta_1) + (2 - 2 \cos \theta_2)$ and $t = 4$ for different h values.

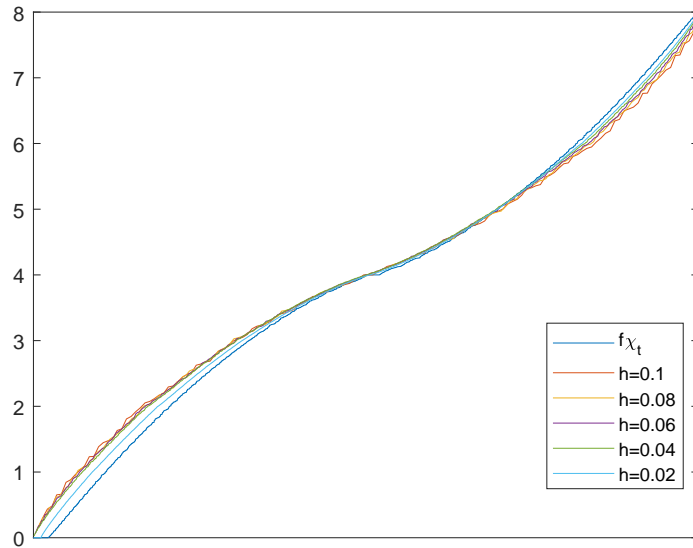


Figure 14: Eigenvalues distribution of $B_{n,t}$ for different h values together with the sampling of $f(\theta_1, \theta_2) = (2 - 2 \cos \theta_1) + (2 - 2 \cos \theta_2)$ and $t = 6$.

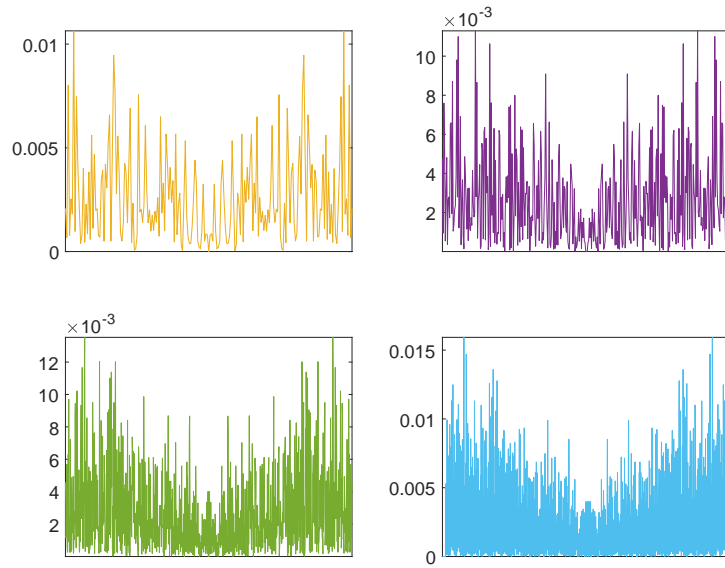


Figure 15: Minimal distance of eigenvalues of $B_{n,t}$ from $f(\theta_1, \theta_2) = (2 - 2 \cos \theta_1) + (2 - 2 \cos \theta_2)$ and $t = 6$ for different h values.

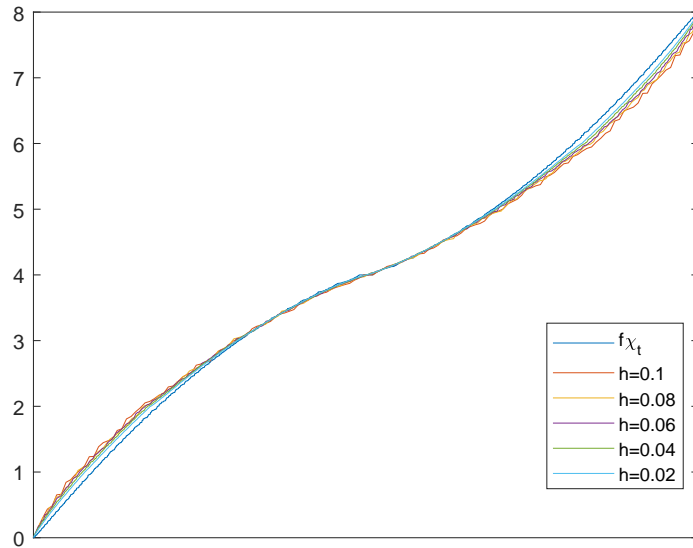


Figure 16: Eigenvalues distribution of $B_{n,t}$ for different h values together with the sampling of $f(\theta_1, \theta_2) = (2 - 2 \cos \theta_1) + (2 - 2 \cos \theta_2)$ and $t = 8$.

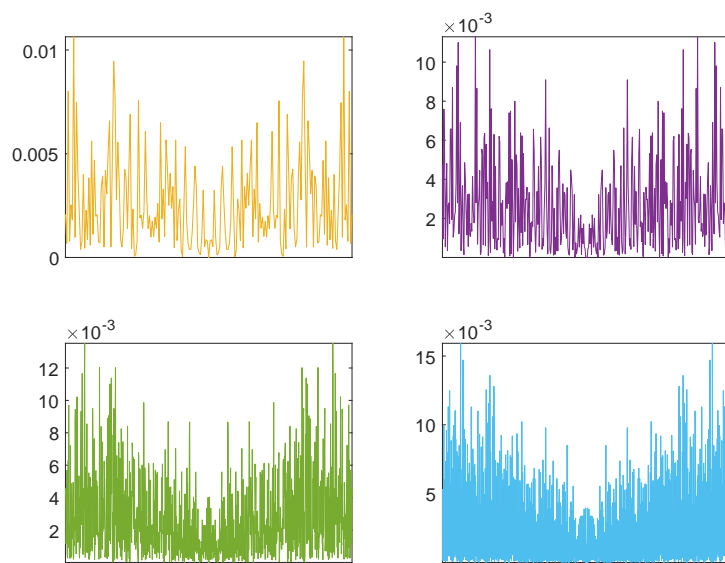


Figure 17: Minimal distance of eigenvalues of $B_{n,t}$ from $f(\theta_1, \theta_2) = (2 - 2 \cos \theta_1) + (2 - 2 \cos \theta_2)$ and $t = 8$ for different h values.

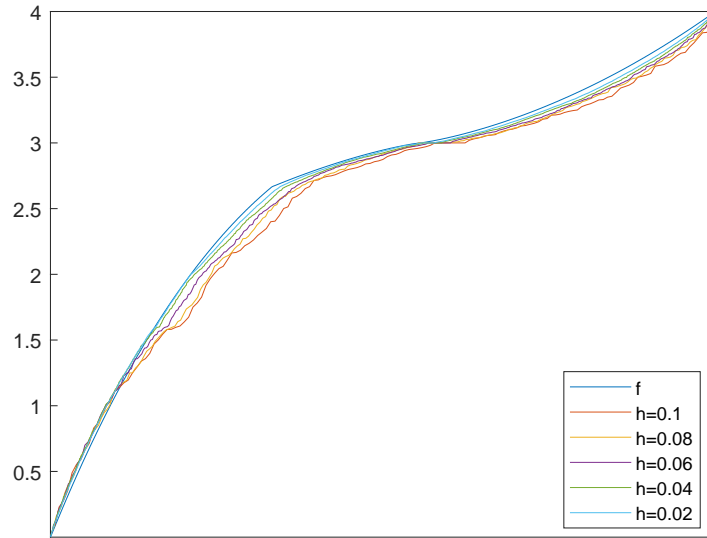


Figure 18: Eigenvalues distribution of A_n for different h values together with the sampling of $f(\theta_1, \theta_2) = (8 - 2 \cos \theta_1 - 2 \cos \theta_2 - 4 \cos \theta_1 \cos \theta_2)/3$.

5.3.2 $Q_1 - f(\theta_1, \theta_2) = (8 - 2 \cos \theta_1 - 2 \cos \theta_2 - 4 \cos \theta_1 \cos \theta_2)/3$

$Q_1: f(\theta_1, \theta_2) = (8 - 2 \cos \theta_1 - 2 \cos \theta_2 - 4 \cos \theta_1 \cos \theta_2)/3$

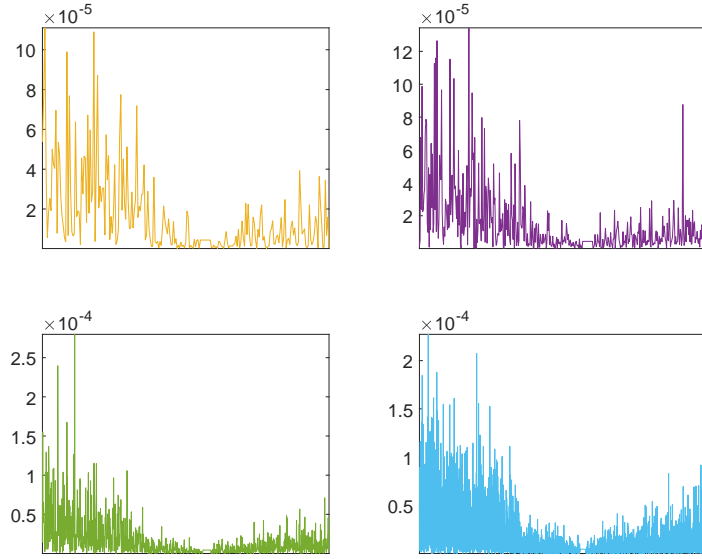


Figure 19: Minimal distance of eigenvalues of A_n from $f(\theta_1, \theta_2) = (8 - 2 \cos \theta_1 - 2 \cos \theta_2 - 4 \cos \theta_1 \cos \theta_2)/3$ for different h values.

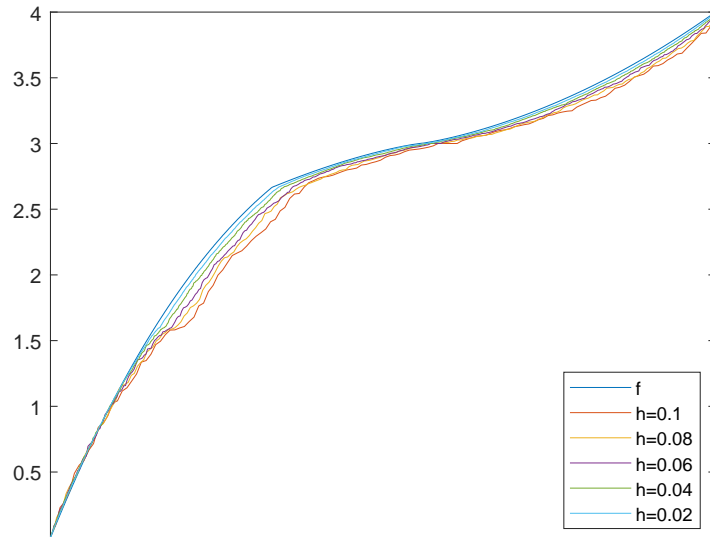


Figure 20: Eigenvalues distribution of $C_{n,t}$ for different h values together with the sampling of $f(\theta_1, \theta_2) = (8 - 2 \cos \theta_1 - 2 \cos \theta_2 - 4 \cos \theta_1 \cos \theta_2)/3$ and $t = 2$.

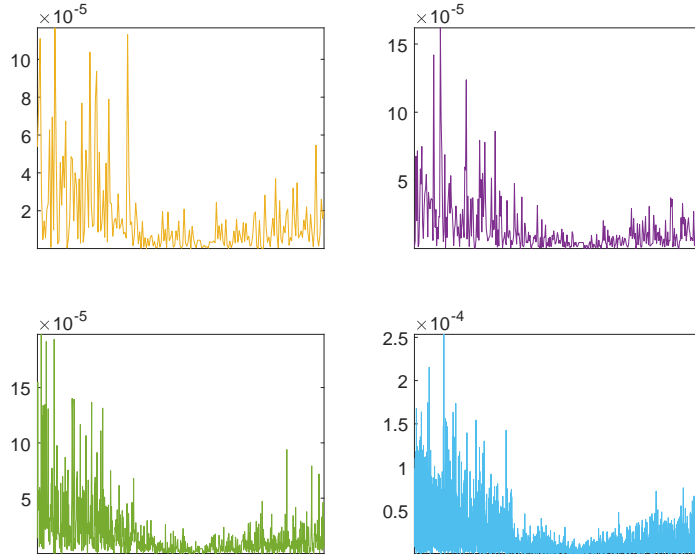


Figure 21: Minimal distance of eigenvalues of $C_{n,t}$ from $f(\theta_1, \theta_2) = (8 - 2 \cos \theta_1 - 2 \cos \theta_2 - 4 \cos \theta_1 \cos \theta_2)/3$ and $t = 2$ for different h values.

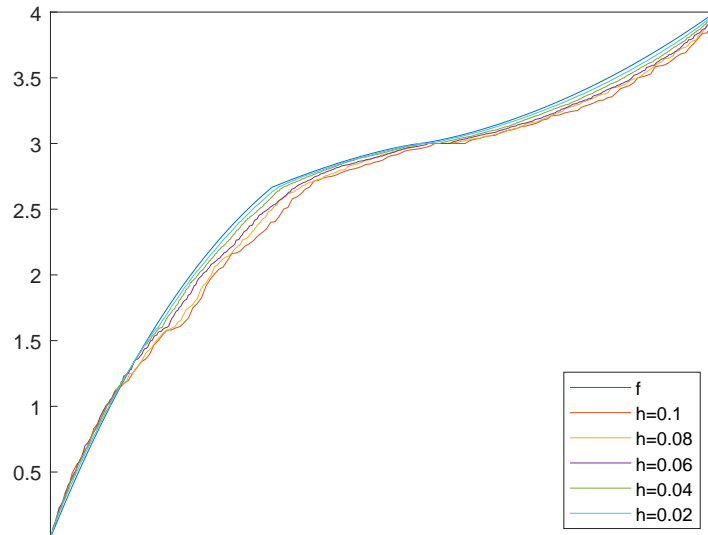


Figure 22: Eigenvalues distribution of $C_{n,t}$ for different h values together with the sampling of $f(\theta_1, \theta_2) = (8 - 2 \cos \theta_1 - 2 \cos \theta_2 - 4 \cos \theta_1 \cos \theta_2)/3$ and $t = 4$.

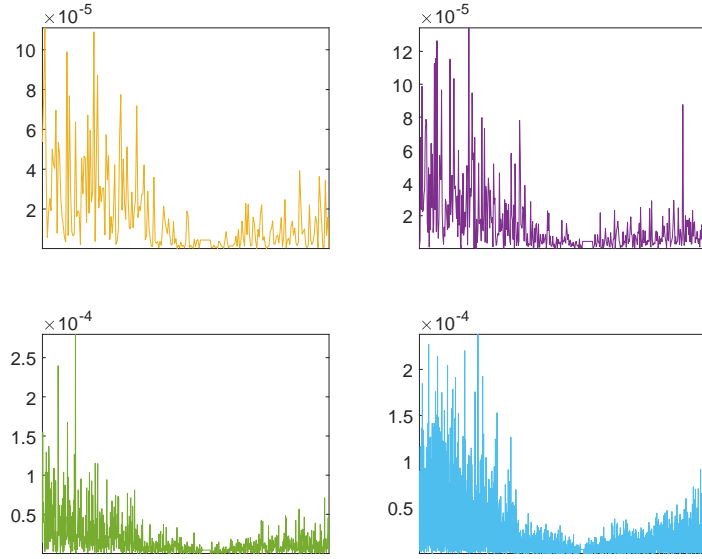


Figure 23: Minimal distance of eigenvalues of $C_{n,t}$ from $f(\theta_1, \theta_2) = (8 - 2 \cos \theta_1 - 2 \cos \theta_2 - 4 \cos \theta_1 \cos \theta_2)/3$ and $t = 4$ for different h values.

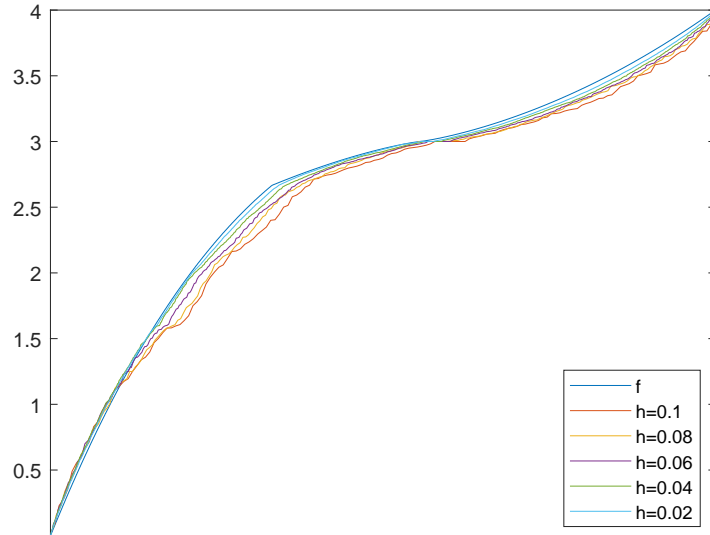


Figure 24: Eigenvalues distribution of $C_{n,t}$ for different h values together with the sampling of $f(\theta_1, \theta_2) = (8 - 2 \cos \theta_1 - 2 \cos \theta_2 - 4 \cos \theta_1 \cos \theta_2)/3$ and $t = 6$.

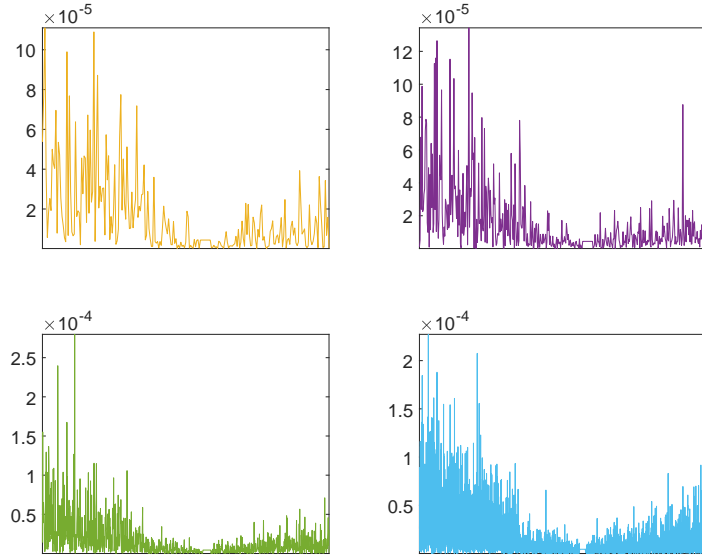


Figure 25: Minimal distance of eigenvalues of $C_{n,t}$ from $f(\theta_1, \theta_2) = (8 - 2 \cos \theta_1 - 2 \cos \theta_2 - 4 \cos \theta_1 \cos \theta_2)/3$ and $t = 6$ for different h values.

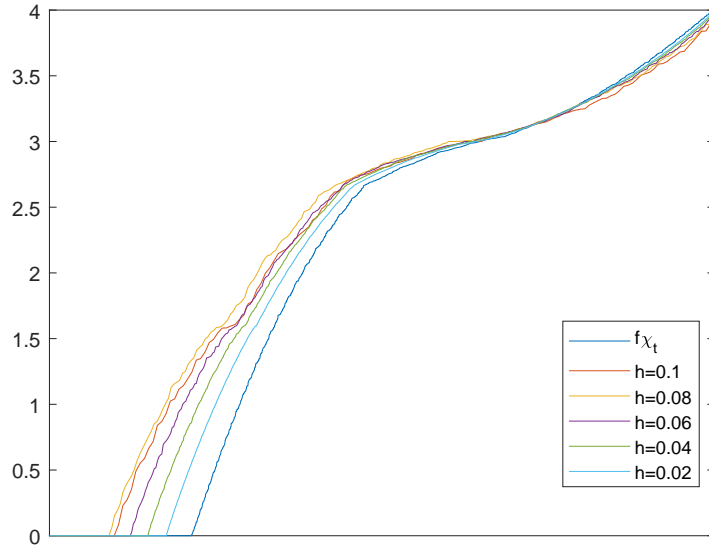


Figure 26: Eigenvalues distribution of $B_{n,t}$ for different h values together with the sampling of $f(\theta_1, \theta_2) = (8 - 2 \cos \theta_1 - 2 \cos \theta_2 - 4 \cos \theta_1 \cos \theta_2)/3$ and $t = 2$.

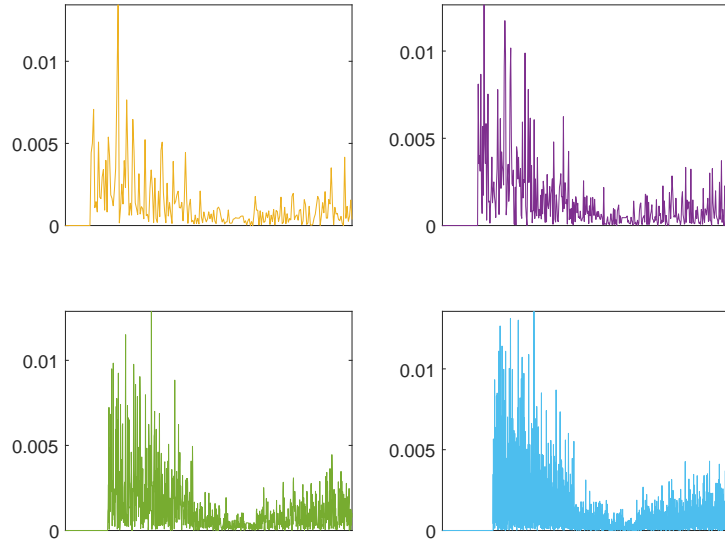


Figure 27: Minimal distance of eigenvalues of $B_{n,t}$ from $f(\theta_1, \theta_2) = (8 - 2 \cos \theta_1 - 2 \cos \theta_2 - 4 \cos \theta_1 \cos \theta_2)/3$ and $t = 2$ for different h values.

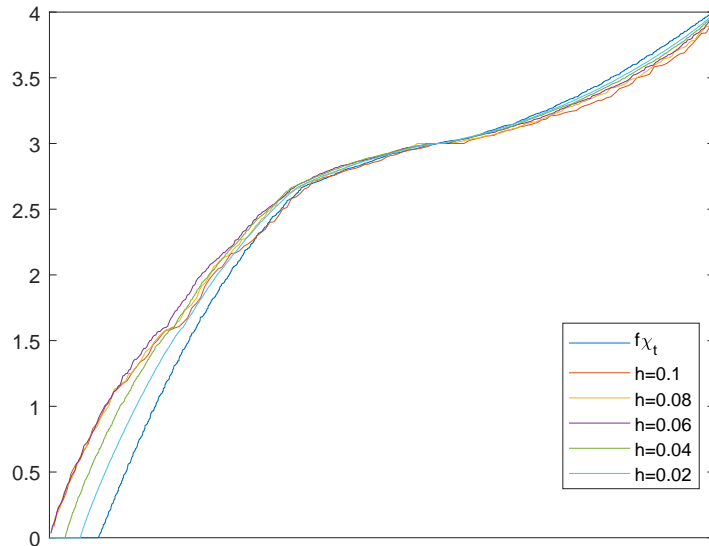


Figure 28: Eigenvalues distribution of $B_{n,t}$ for different h values together with the sampling of $f(\theta_1, \theta_2) = (8 - 2 \cos \theta_1 - 2 \cos \theta_2 - 4 \cos \theta_1 \cos \theta_2)/3$ and $t = 4$.

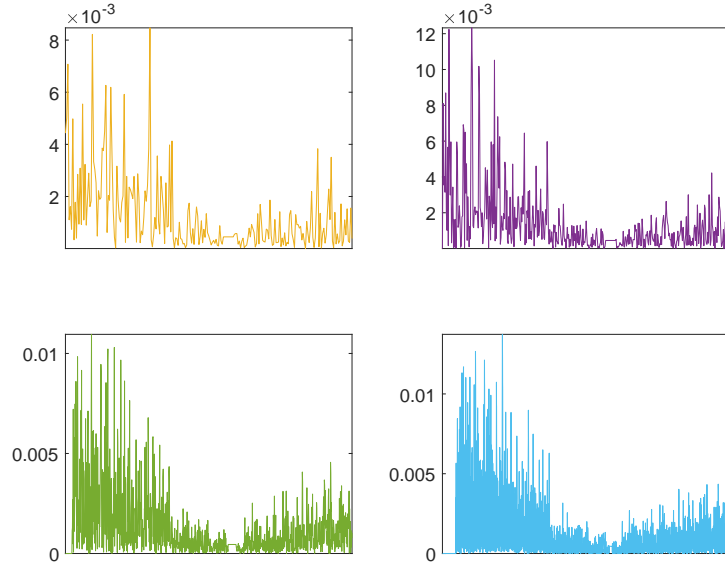


Figure 29: Minimal distance of eigenvalues of $B_{n,t}$ from $f(\theta_1, \theta_2) = (8 - 2 \cos \theta_1 - 2 \cos \theta_2 - 4 \cos \theta_1 \cos \theta_2)/3$ and $t = 4$ for different h values.

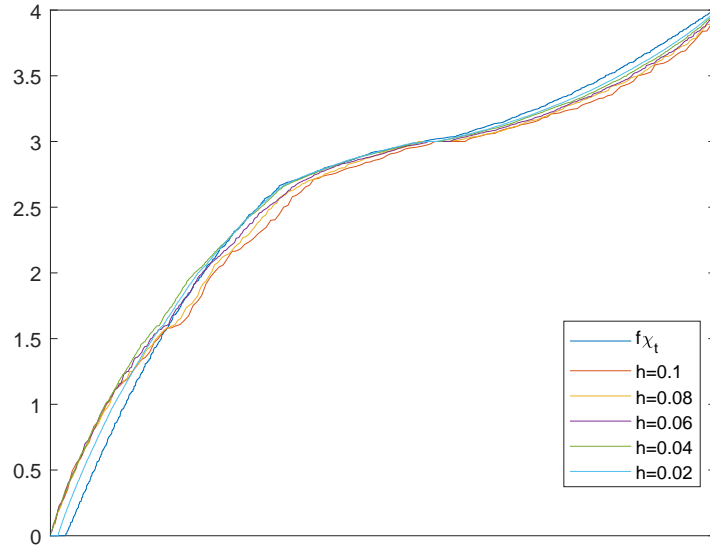


Figure 30: Eigenvalues distribution of $B_{n,t}$ for different h values together with the sampling of $f(\theta_1, \theta_2) = (8 - 2 \cos \theta_1 - 2 \cos \theta_2 - 4 \cos \theta_1 \cos \theta_2)/3$ and $t = 6$.

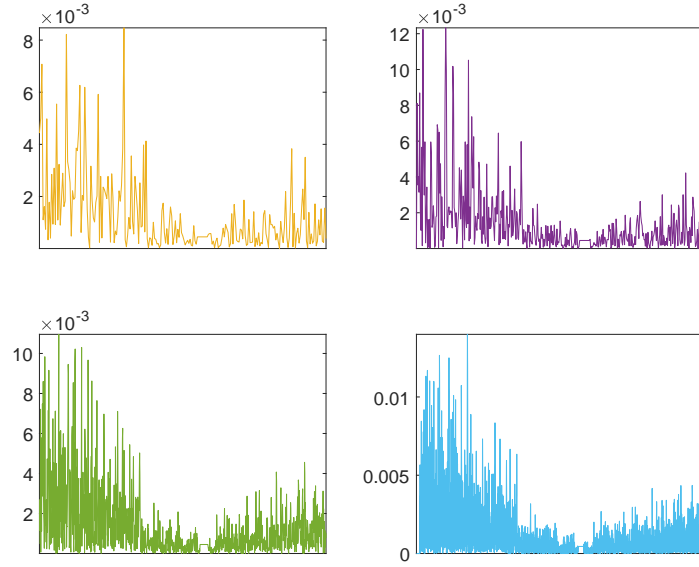


Figure 31: Minimal distance of eigenvalues of $B_{n,t}$ from $f(\theta_1, \theta_2) = (8 - 2 \cos \theta_1 - 2 \cos \theta_2 - 4 \cos \theta_1 \cos \theta_2)/3$ and $t = 6$ for different h values.

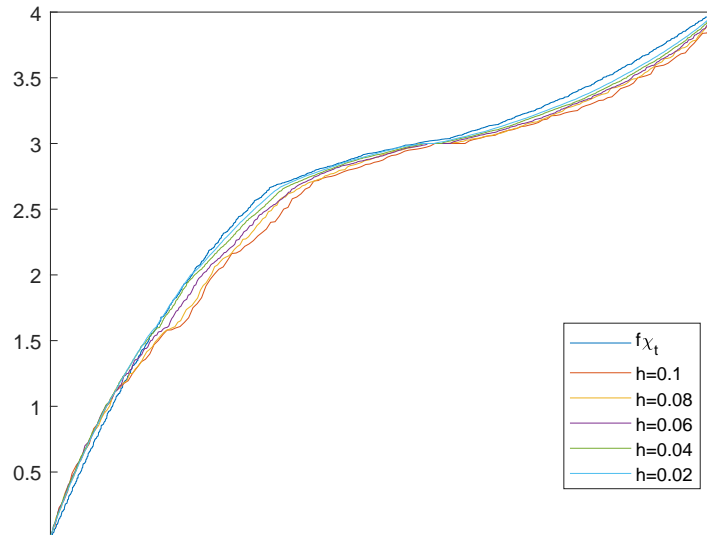


Figure 32: Eigenvalues distribution of $B_{n,t}$ for different h values together with the sampling of $f(\theta_1, \theta_2) = (8 - 2 \cos \theta_1 - 2 \cos \theta_2 - 4 \cos \theta_1 \cos \theta_2)/3$ and $t = 8$.

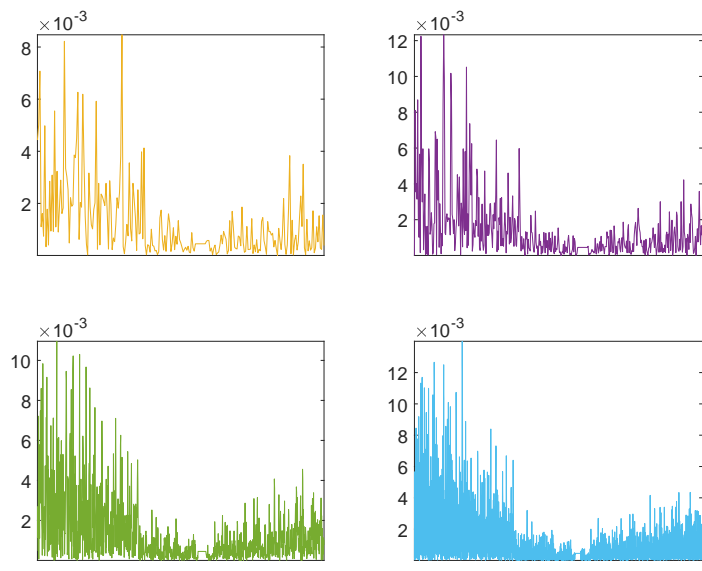


Figure 33: Minimal distance of eigenvalues of $B_{n,t}$ from $f(\theta_1, \theta_2) = (8 - 2 \cos \theta_1 - 2 \cos \theta_2 - 4 \cos \theta_1 \cos \theta_2)/3$ and $t = 8$ for different h values.

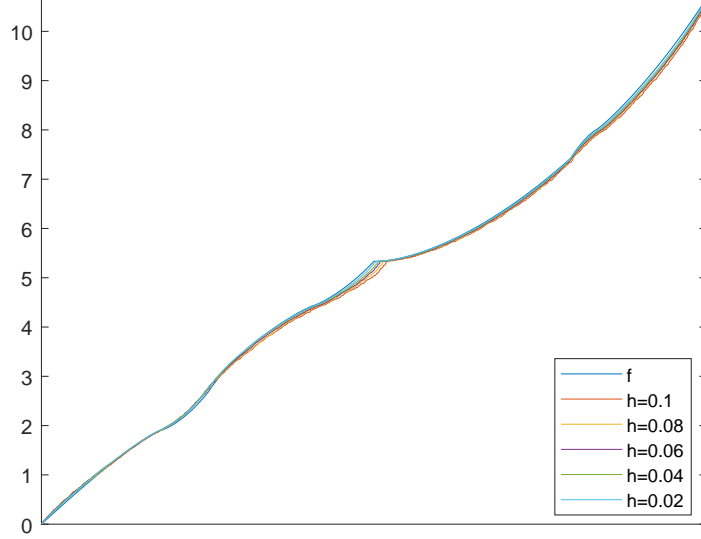


Figure 34: Eigenvalues distribution of A_n for different h values together with the sampling of $f(\theta_1, \theta_2) = f_{P_2}(\theta_1, \theta_2)$.

5.3.3 $P_2 - f_{P_2} : [-\pi, \pi]^2 \longrightarrow \mathbb{C}^{4 \times 4}$

P_2 : Matrix-valued symbol $f_{P_2} : [-\pi, \pi]^2 \longrightarrow \mathbb{C}^{4 \times 4}$ with

$$f_{P_2}(\theta_1, \theta_2) = \left[\begin{array}{cc|cc} \alpha & -\beta(1 + e^{i\theta_1}) & -\beta(1 + e^{i\theta_2}) & 0 \\ -\beta(1 + e^{-i\theta_1}) & \alpha & 0 & -\beta(1 + e^{i\theta_2}) \\ \hline -\beta(1 + e^{-i\theta_2}) & 0 & \alpha & -\beta(1 + e^{i\theta_1}) \\ 0 & -\beta(1 + e^{-i\theta_2}) & -\beta(1 + e^{-i\theta_1}) & \gamma + \frac{\beta}{2}(\cos(\theta_1) + \cos(\theta_2)) \end{array} \right] \quad (17)$$

with $\alpha = 16/3$, $\beta = 4/3$, and $\gamma = 4$.

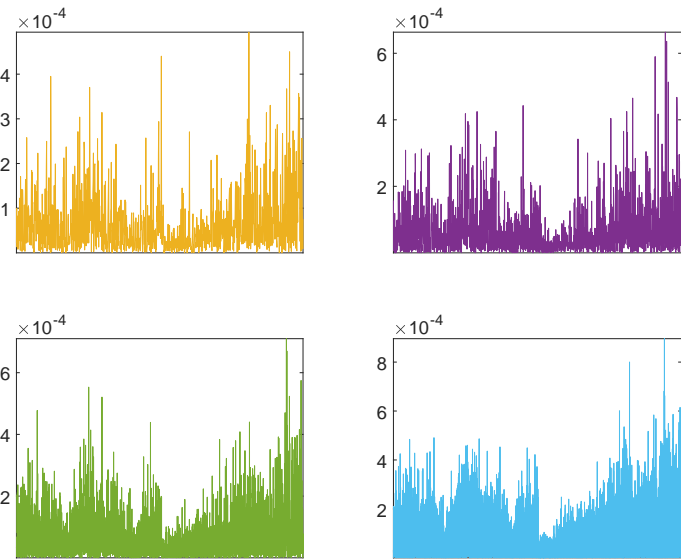


Figure 35: Minimal distance of eigenvalues of A_n from $f(\theta_1, \theta_2) = f_{P_2}(\theta_1, \theta_2)$ for different h values.

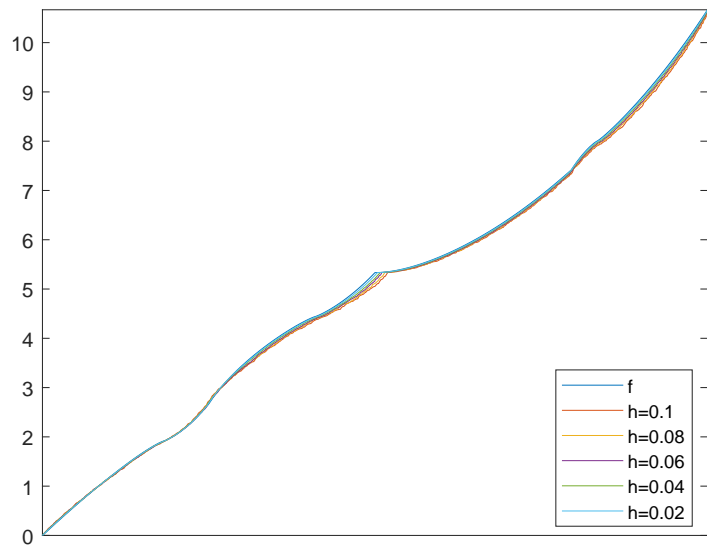


Figure 36: Eigenvalues distribution of $C_{n,t}$ for different h values together with the sampling of $f(\theta_1, \theta_2) = f_{P_2}(\theta_1, \theta_2)$ and $t = 2$.

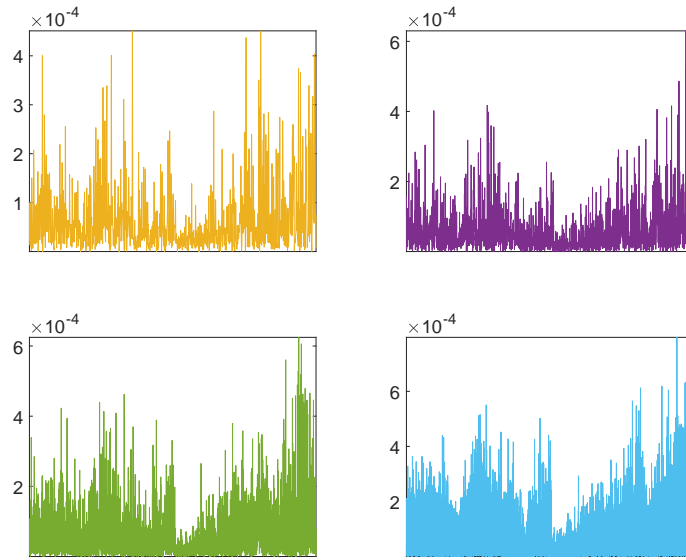


Figure 37: Minimal distance of eigenvalues of $C_{n,t}$ from $f(\theta_1, \theta_2) = f_{P_2}(\theta_1, \theta_2)$ and $t = 2$ for different h values.

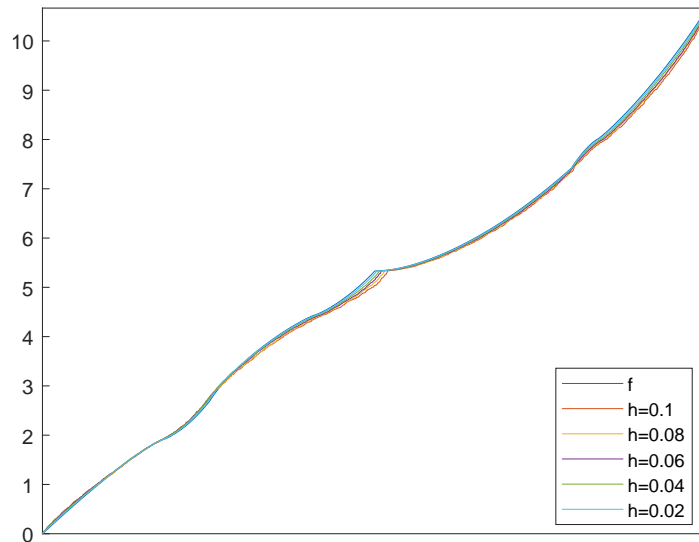


Figure 38: Eigenvalues distribution of $C_{n,t}$ for different h values together with the sampling of $f(\theta_1, \theta_2) = f_{P_2}(\theta_1, \theta_2)$ and $t = 4$.

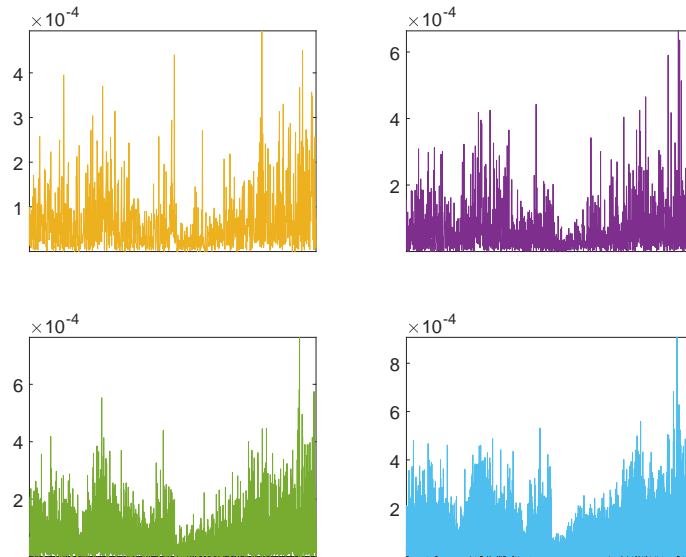


Figure 39: Minimal distance of eigenvalues of $C_{n,t}$ from $f(\theta_1, \theta_2) = f_{P_2}(\theta_1, \theta_2)$ and $t = 4$ for different h values.

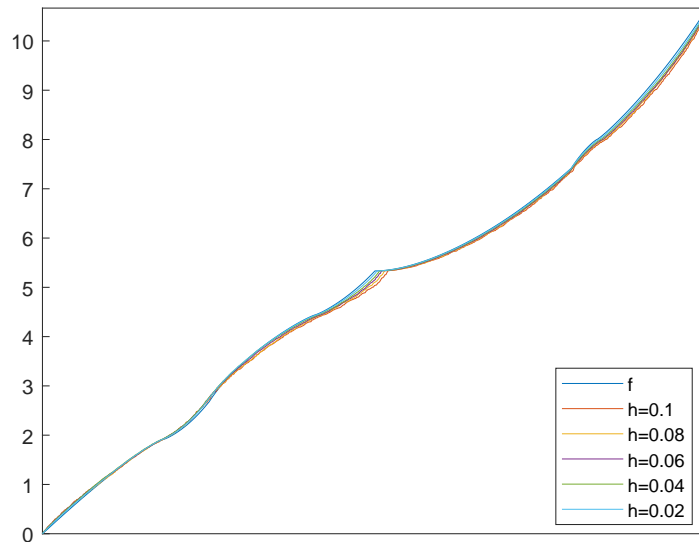


Figure 40: Eigenvalues distribution of $C_{n,t}$ for different h values together with the sampling of $f(\theta_1, \theta_2) = f_{P_2}(\theta_1, \theta_2)$ and $t = 6$.

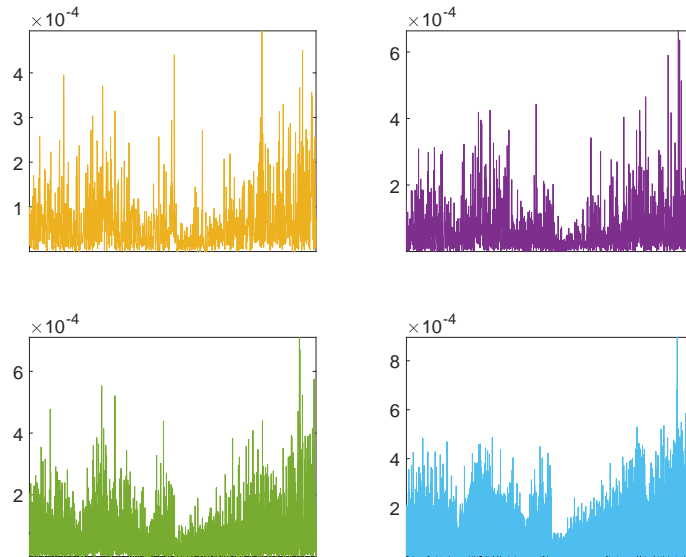


Figure 41: Minimal distance of eigenvalues of $C_{n,t}$ from $f(\theta_1, \theta_2) = f_{P_2}(\theta_1, \theta_2)$ and $t = 6$ for different h values.

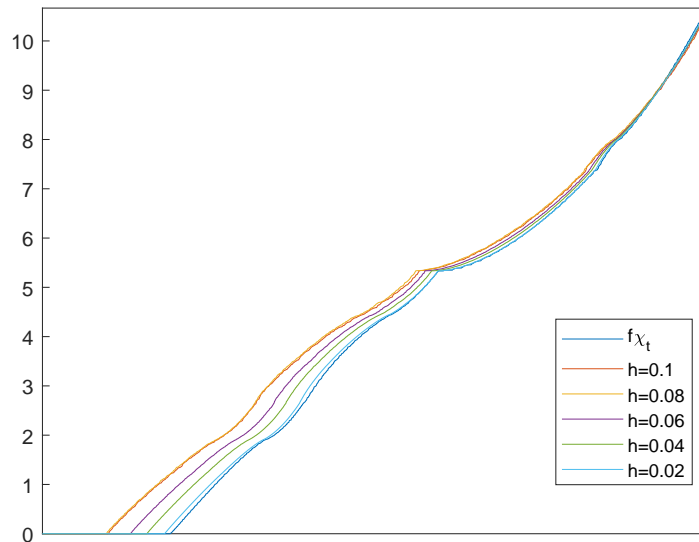


Figure 42: Eigenvalues distribution of $B_{n,t}$ for different h values together with the sampling of $f(\theta_1, \theta_2) = f_{P_2}(\theta_1, \theta_2)$ and $t = 2$.

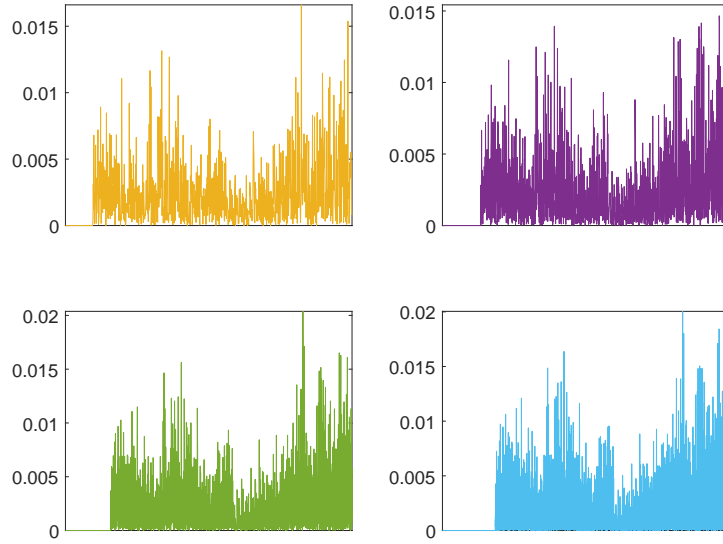


Figure 43: Minimal distance of eigenvalues of $B_{n,t}$ from $f(\theta_1, \theta_2) = f_{P_2}(\theta_1, \theta_2)$ and $t = 2$ for different h values.

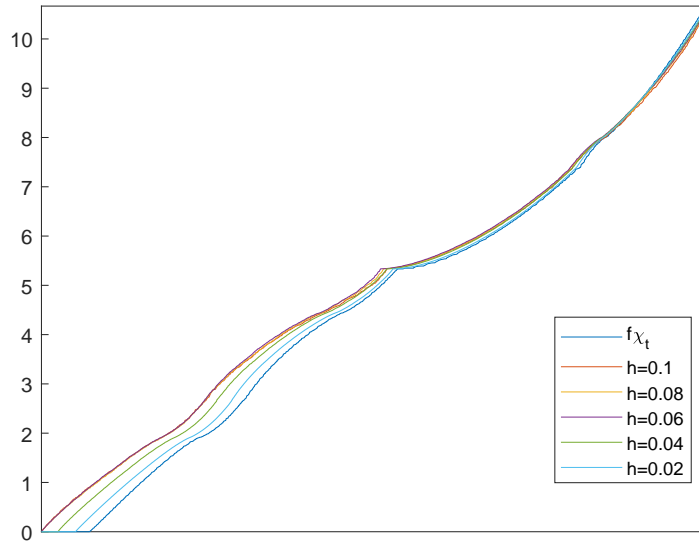


Figure 44: Eigenvalues distribution of $B_{n,t}$ for different h values together with the sampling of $f(\theta_1, \theta_2) = f_{P_2}(\theta_1, \theta_2)$ and $t = 4$.

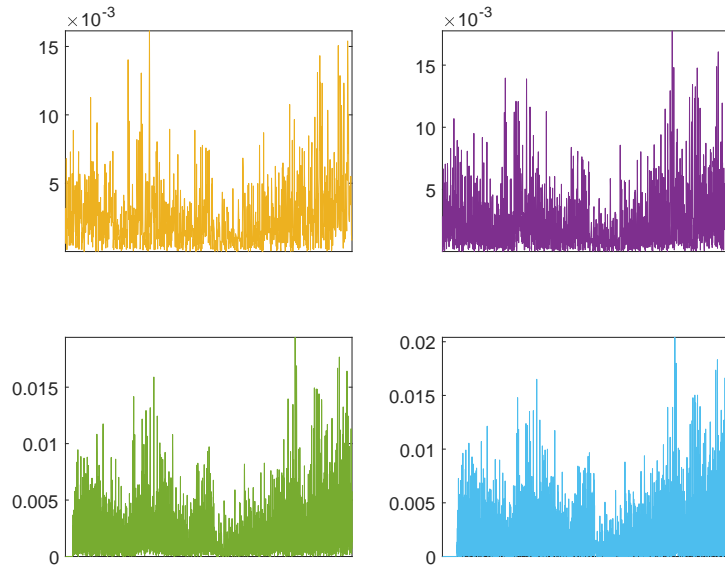


Figure 45: Minimal distance of eigenvalues of $B_{n,t}$ from $f(\theta_1, \theta_2) = f_{P_2}(\theta_1, \theta_2)$ and $t = 4$ for different h values.

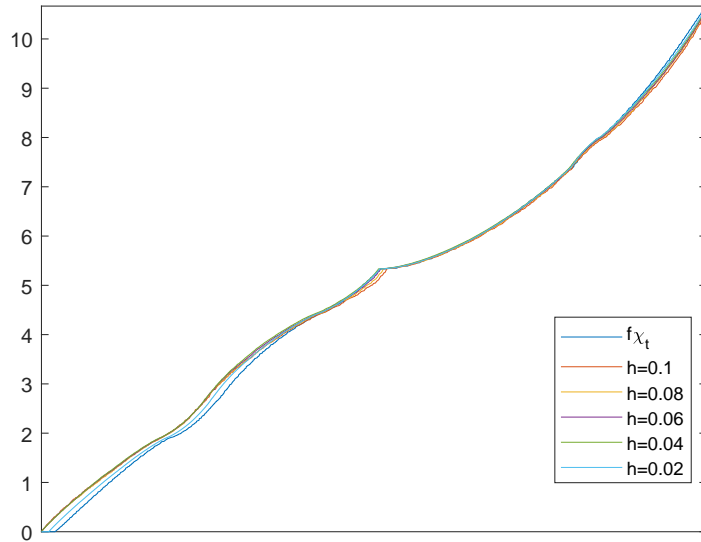


Figure 46: Eigenvalues distribution of $B_{n,t}$ for different h values together with the sampling of $f(\theta_1, \theta_2) = f_{P_2}(\theta_1, \theta_2)$ and $t = 6$.

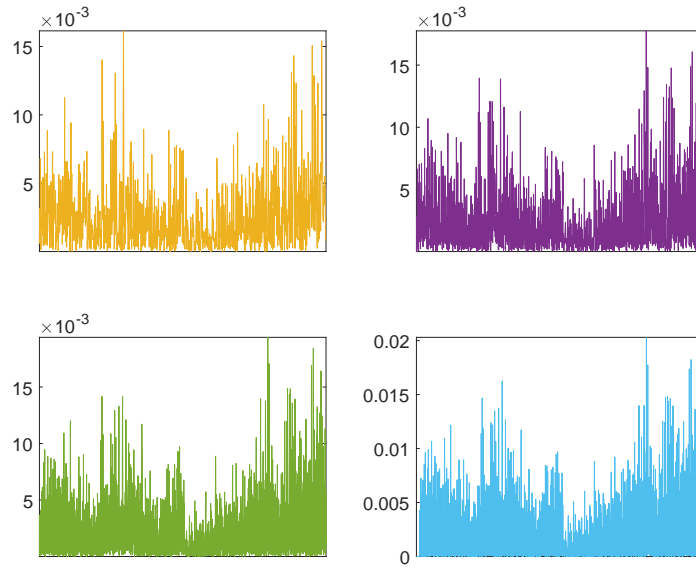


Figure 47: Minimal distance of eigenvalues of $B_{n,t}$ from $f(\theta_1, \theta_2) = f_{P_2}(\theta_1, \theta_2)$ and $t = 6$ for different h values.

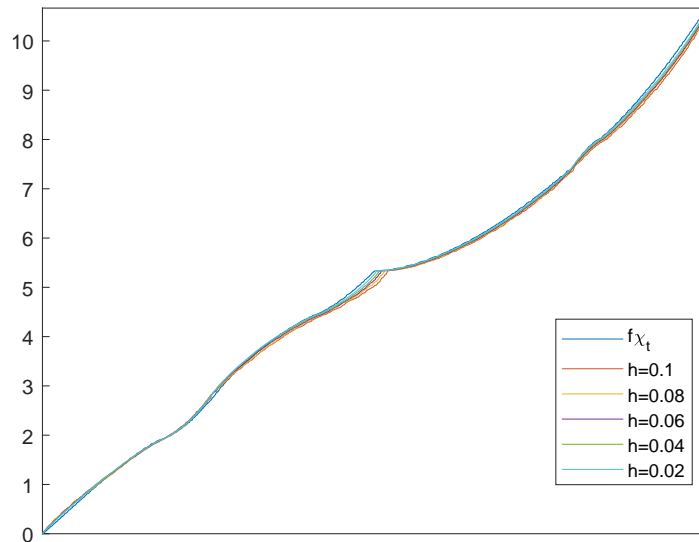


Figure 48: Eigenvalues distribution of $B_{n,t}$ for different h values together with the sampling of $f(\theta_1, \theta_2) = f_{P_2}(\theta_1, \theta_2)$ and $t = 8$.

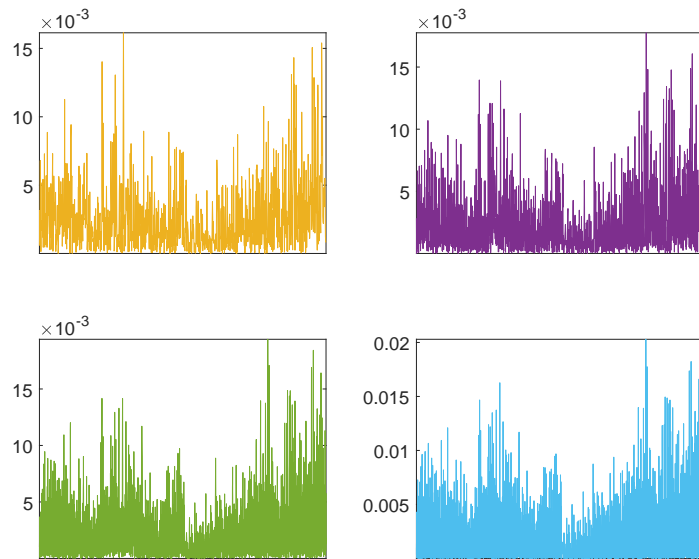


Figure 49: Minimal distance of eigenvalues of $B_{n,t}$ from $f(\theta_1, \theta_2) = f_{P_2}(\theta_1, \theta_2)$ and $t = 8$ for different h values.

6 $P_1 - f(\theta_1, \theta_2) = (2 - 2 \cos \theta_1) + (2 - 2 \cos \theta_2)$ **variable coefficient**

$$P_1: f(\theta_1, \theta_2, x, y) = [(2 - 2 \cos \theta_1) + (2 - 2 \cos \theta_2)]a(x, y)$$

$$a(x, y) = (10 + x^2 + 2y^2 + \sin^2(x + y))/(1 + x^2 + y^2)$$

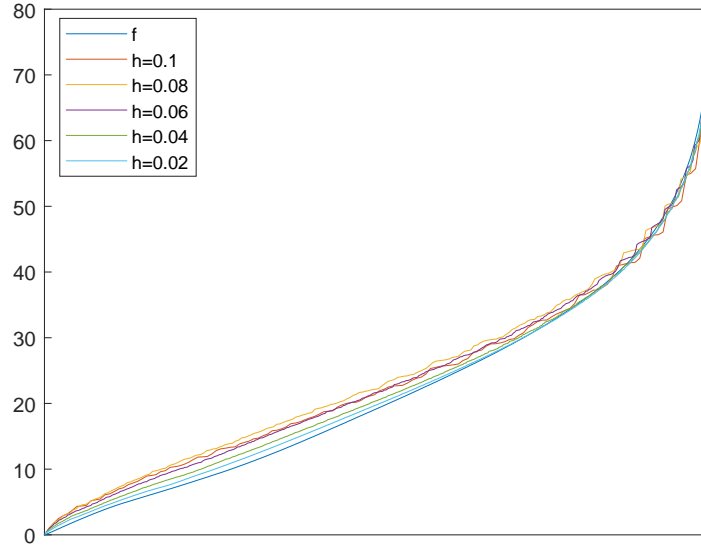


Figure 50: Eigenvalues distribution of $A_n(a)$ for different h values together with the sampling of $f(\theta_1, \theta_2, x, y) = [(2 - 2 \cos \theta_1) + (2 - 2 \cos \theta_2)]a(x, y)$.

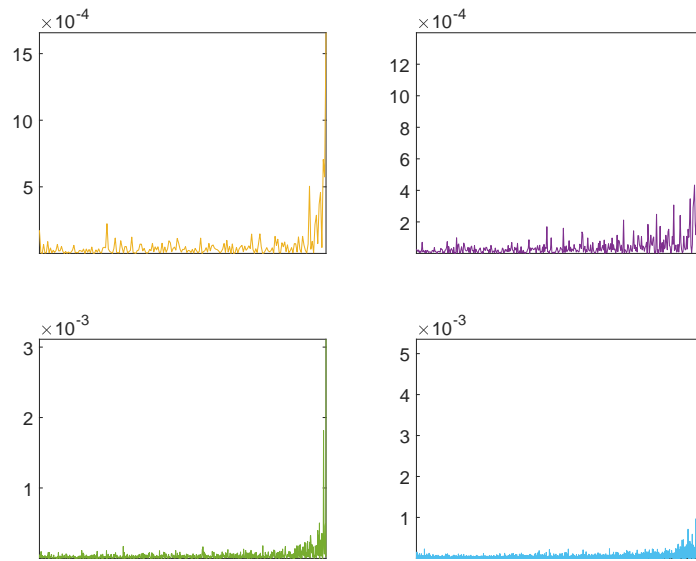


Figure 51: Minimal distance of eigenvalues of $A_n(a)$ from $f(\theta_1, \theta_2, x, y) = [(2 - 2 \cos \theta_1) + (2 - 2 \cos \theta_2)]a(x, y)$ for different h values.

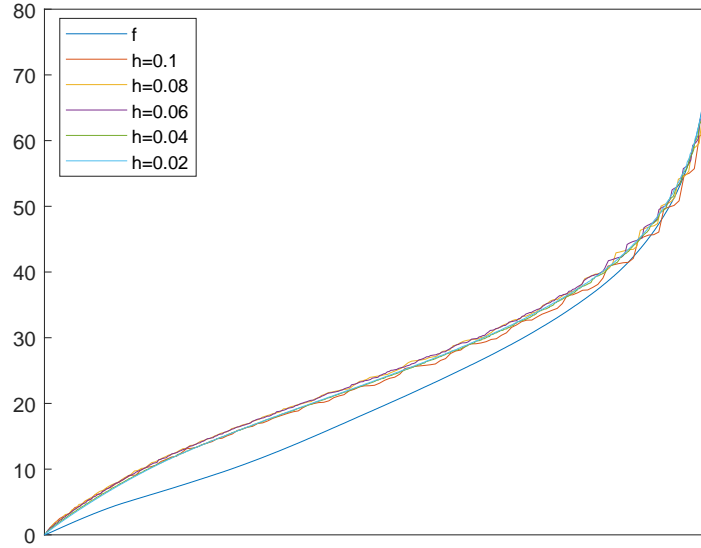


Figure 52: Eigenvalues distribution of $C_{n,t}(a)$ for different h values together with the sampling of $f(\theta_1, \theta_2, x, y) = [(2 - 2 \cos \theta_1) + (2 - 2 \cos \theta_2)]a(x, y)$ and $t = 2$.

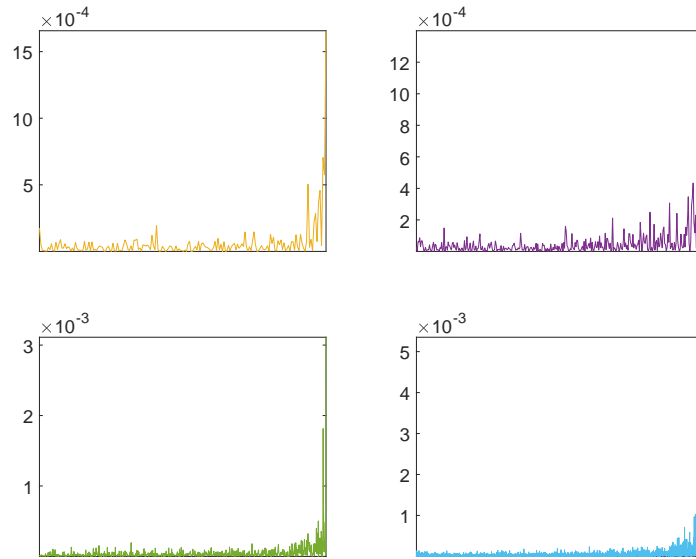


Figure 53: Minimal distance of eigenvalues of $C_{n,t}(a)$ from $f(\theta_1, \theta_2, x, y) = [(2 - 2 \cos \theta_1) + (2 - 2 \cos \theta_2)]a(x, y)$ and $t = 2$ for different h values.

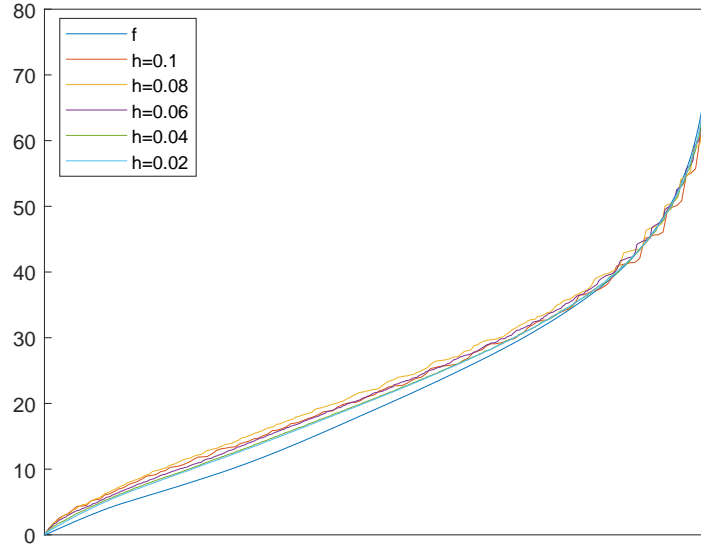


Figure 54: Eigenvalues distribution of $C_{n,t}(a)$ for different h values together with the sampling of $f(\theta_1, \theta_2, x, y) = [(2 - 2 \cos \theta_1) + (2 - 2 \cos \theta_2)]a(x, y)$ and $t = 4$.

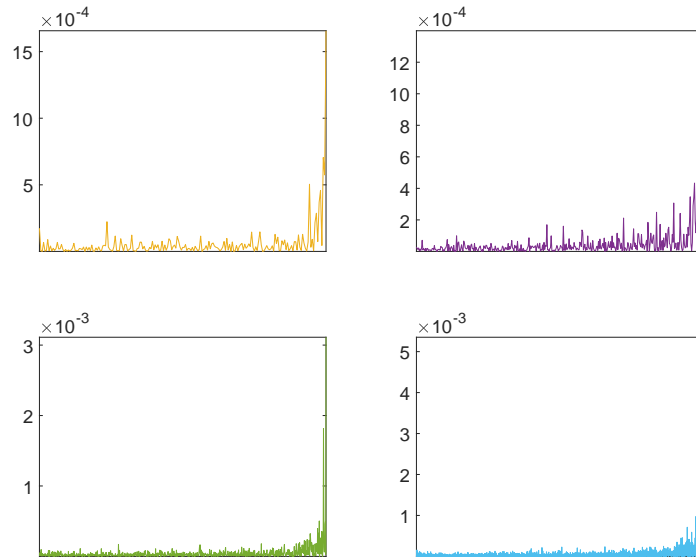


Figure 55: Minimal distance of eigenvalues of $C_{n,t}(a)$ from $f(\theta_1, \theta_2, x, y) = [(2 - 2 \cos \theta_1) + (2 - 2 \cos \theta_2)]a(x, y)$ and $t = 4$ for different h values.

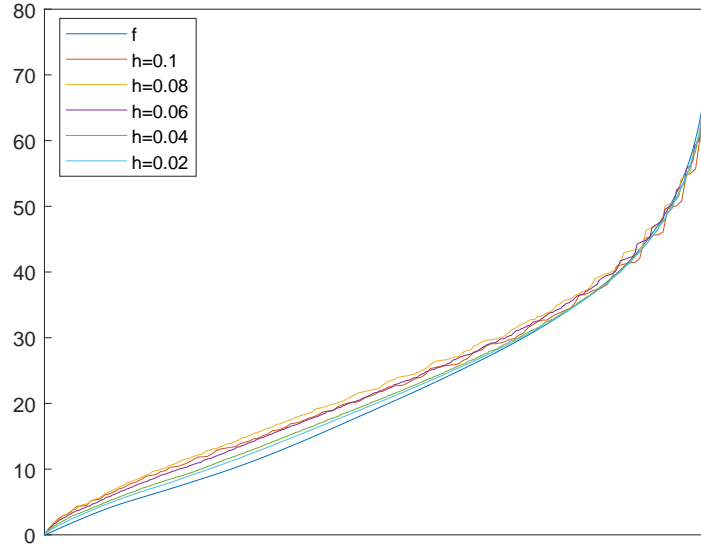


Figure 56: Eigenvalues distribution of $C_{n,t}(a)$ for different h values together with the sampling of $f(\theta_1, \theta_2, x, y) = [(2 - 2 \cos \theta_1) + (2 - 2 \cos \theta_2)]a(x, y)$ and $t = 6$.

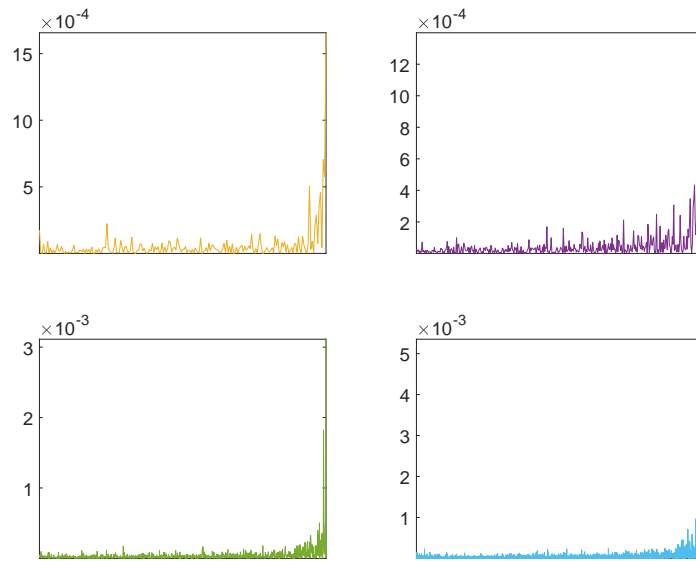


Figure 57: Minimal distance of eigenvalues of $C_{n,t}(a)$ from $f(\theta_1, \theta_2, x, y) = [(2 - 2 \cos \theta_1) + (2 - 2 \cos \theta_2)]a(x, y)$ and $t = 6$ for different h values.

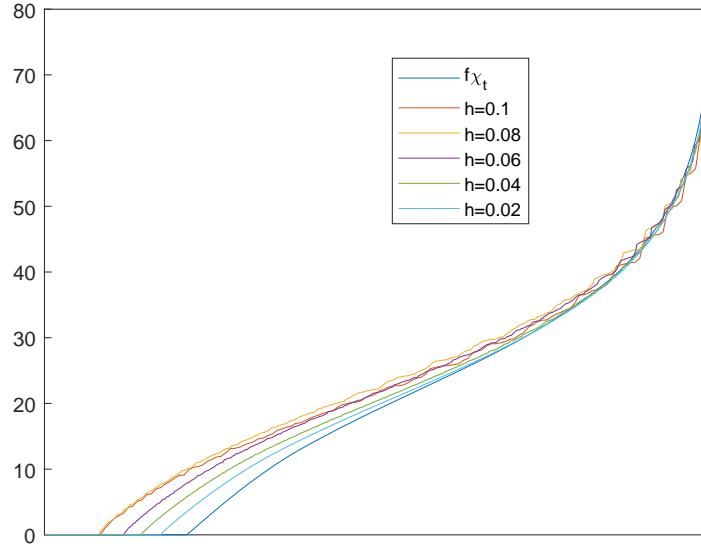


Figure 58: Eigenvalues distribution of $B_{n,t}(a)$ for different h values together with the sampling of $f(\theta_1, \theta_2, x, y) = [(2 - 2 \cos \theta_1) + (2 - 2 \cos \theta_2)]a(x, y)$ and $t = 2$.

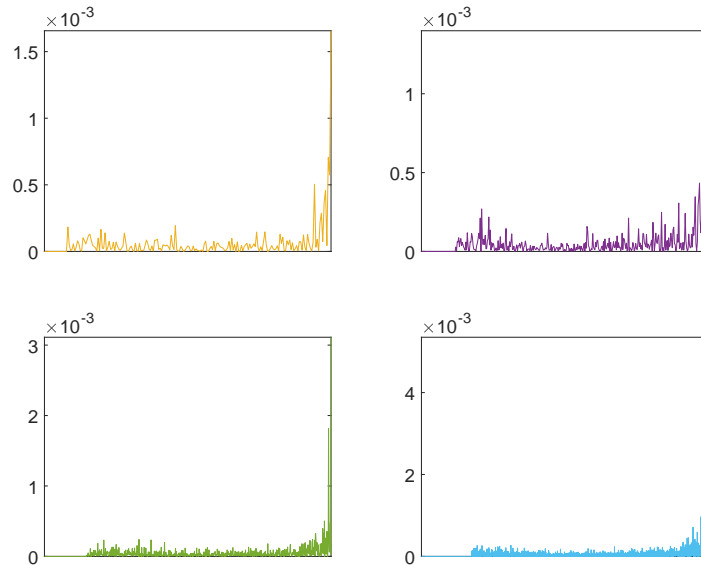


Figure 59: Minimal distance of eigenvalues of $B_{n,t}(a)$ from $f(\theta_1, \theta_2, x, y) = [(2 - 2 \cos \theta_1) + (2 - 2 \cos \theta_2)]a(x, y)$ and $t = 2$ for different h values.

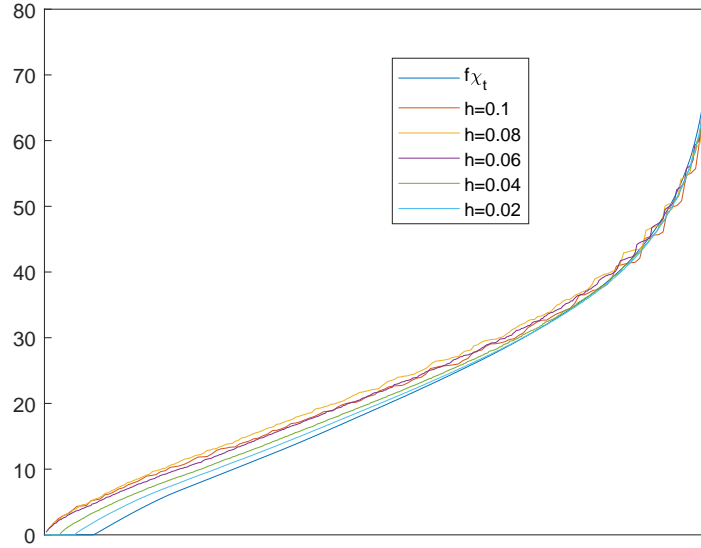


Figure 60: Eigenvalues distribution of $B_{n,t}(a)$ for different h values together with the sampling of $f(\theta_1, \theta_2, x, y) = [(2 - 2 \cos \theta_1) + (2 - 2 \cos \theta_2)]a(x, y)$ and $t = 4$.

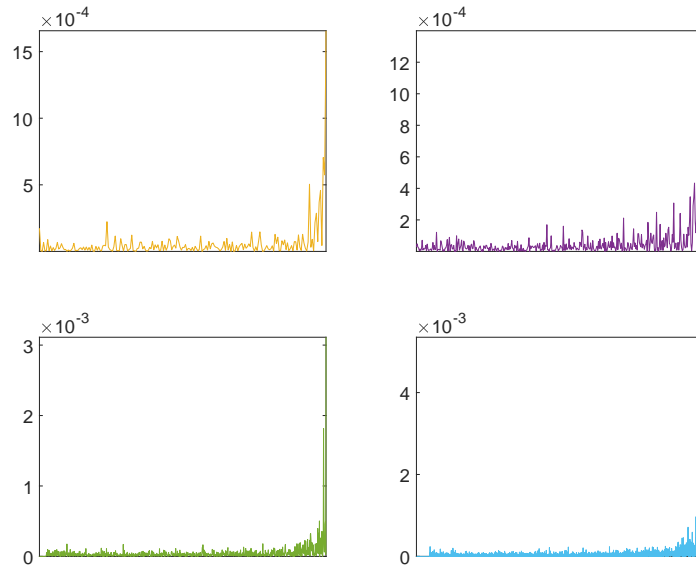


Figure 61: Minimal distance of eigenvalues of $B_{n,t}(a)$ from $f(\theta_1, \theta_2, x, y) = [(2 - 2 \cos \theta_1) + (2 - 2 \cos \theta_2)]a(x, y)$ and $t = 4$ for different h values.

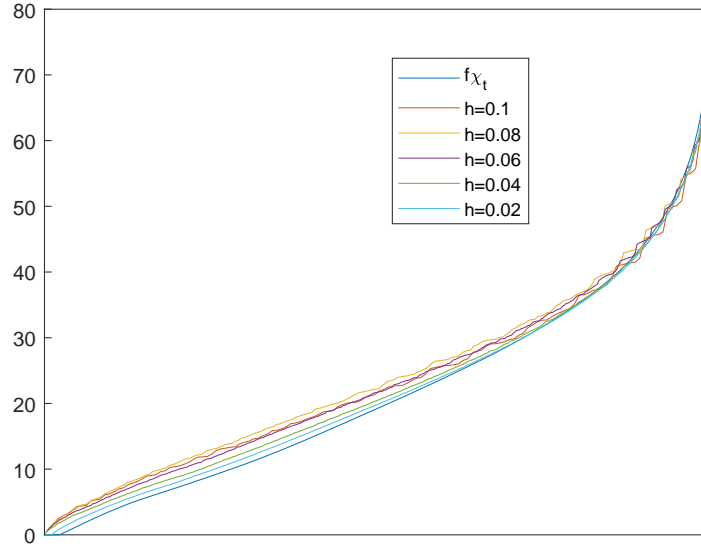


Figure 62: Eigenvalues distribution of $B_{n,t}(a)$ for different h values together with the sampling of $f(\theta_1, \theta_2, x, y) = [(2 - 2 \cos \theta_1) + (2 - 2 \cos \theta_2)]a(x, y)$ and $t = 6$.

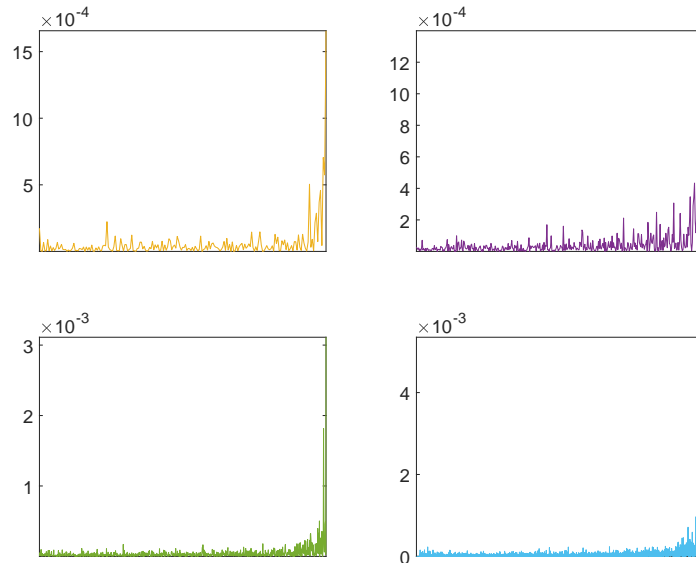


Figure 63: Minimal distance of eigenvalues of $B_{n,t}(a)$ from $f(\theta_1, \theta_2, x, y) = [(2 - 2 \cos \theta_1) + (2 - 2 \cos \theta_2)]a(x, y)$ and $t = 6$ for different h values.

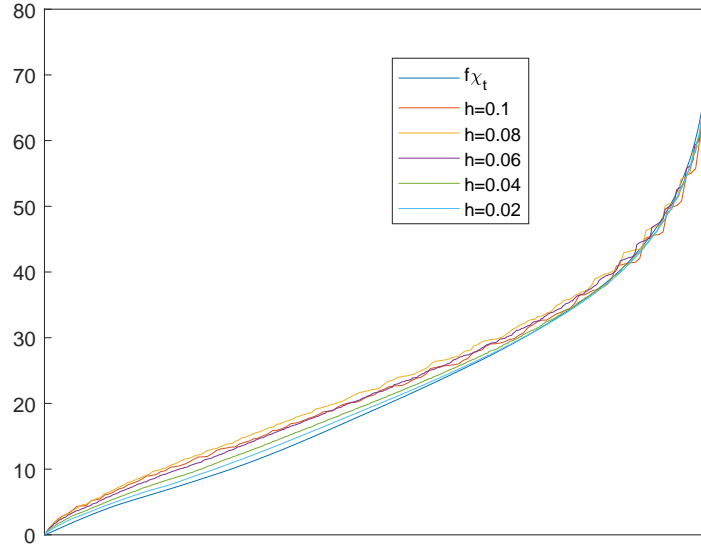


Figure 64: Eigenvalues distribution of $B_{n,t}(a)$ for different h values together with the sampling of $f(\theta_1, \theta_2, x, y) = [(2 - 2 \cos \theta_1) + (2 - 2 \cos \theta_2)]a(x, y)$ and $t = 8$.

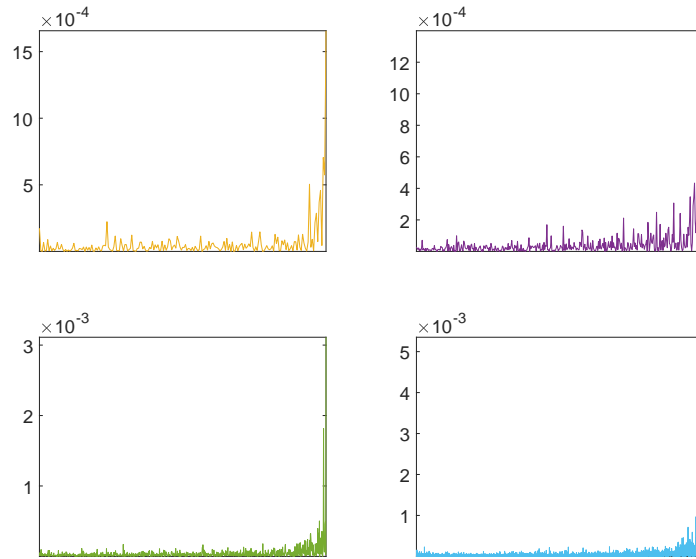


Figure 65: Minimal distance of eigenvalues of $B_{n,t}(a)$ from $f(\theta_1, \theta_2, x, y) = [(2 - 2 \cos \theta_1) + (2 - 2 \cos \theta_2)]a(x, y)$ and $t = 8$ for different h values.

7 Conclusions

We considered matrix-sequences $\{B_{n,t}\}_n$ of increasing sizes depending on n and equipped with a parameter $t > 0$. For every fixed $t > 0$, we assumed that each $\{B_{n,t}\}_n$ possesses a canonical spectral/singular values symbol f_t defined on $D_t \subset \mathbb{R}^d$ of finite measure, $d \geq 1$. Furthermore we assumed that $\{\{B_{n,t}\} : t > 0\}$ is an a.c.s. for $\{A_n\}$ and that $\bigcup_{t>0} D_t = D$ with $D_{t+1} \supset D_t$. Under such assumptions and via the a.c.s. notion, we proved general distribution results on the canonical distributions of $\{A_n\}$, whose symbol, when it exists, can be defined on the possibly unbounded domain D of finite or even infinite measure. In a second theoretical part, we concentrated our attention on the case of unbounded domains of finite measure and we introduce a new concept, the g.a.c.s., which is suited particularly when moving or unbounded domains have to be treated.

Beside the notions of a.c.s and g.a.c.s, the main tool in concrete applications is the theory of GLT matrix-sequences to which usually all the basic matrix-sequences $\{B_{n,t}\}_n$ belong for every $t > 0$, as shown in the examples stemming from the numerical approximation of PDEs/FDEs with either moving or unbounded domains. Several numerical evidences have been given in order to corroborate the analysis.

As open questions we can mention the following main items:

1. In the present work we focused on the case of unbounded domains with finite measure. However, as already mentioned, the problem of dealing with discretizations on domains of infinite measure remains interesting, both from the point of view of approximation and from the distributional point of view. In this context, also using the simpler a.c.s. notion, there is probably not a distributional symbol for the sequence as in the classical sense, but rather a limit operator α which exploits some features of the discretized operator.
2. The a.c.s. notion has been used as one of the main tools at the foundation of the GLT theory. It is possible that a similar role could be played by the notion of g.a.c.s. for the construction of a new large class of sequences. This will be subject of further study in the future.
3. The study of the eigenvalue distribution in non-normal cases in which the matrix-sequence cannot be viewed as a small perturbation of a Hermitian matrix-sequence is still very intricate (see [36, 37, 32] and the use of potential theory in [35] and references therein). This type of research is very challenging/difficult and it is worth to be considered.

Declarations

Conflict of Interests The authors declare that they have no conflict of interest.

Contribution The authors have all contributed equally to the present work.

Acknowledgments

The research of all the authors was partly supported by the Italian INdAM-GNCS agency. Furthermore, the work of Stefano Serra-Capizzano was funded from the European High-Performance Computing Joint Undertaking (JU) under grant agreement No 955701. The JU receives support from the European Union's Horizon 2020 research and innovation programme and Belgium, France, Germany, Switzerland. Furthermore Stefano Serra-Capizzano is grateful for the support of the Laboratory of Theory, Economics and Systems – Department of Computer Science at Athens University of Economics and Business.

References

- [1] A. Adriani, M. Semplice, and S. Serra-Capizzano, *Generalized Locally Toeplitz matrix-sequences and approximated PDEs on submanifolds: the flat case*, Linear Multilin. Algebra (2023); online 27-9-23.
- [2] G. Barbarino, *A systematic approach to reduced GLT*, BIT Numer. Math. 62.3 (2022), pp. 681–743.
- [3] G. Barbarino, C. Garoni, and S. Serra-Capizzano, *Block generalized locally Toeplitz sequences: theory and applications in the unidimensional case*, Electron. Trans. Numer. Anal. 53 (2020), pp. 28–112.
- [4] G. Barbarino, C. Garoni, and S. Serra-Capizzano, *Block generalized locally Toeplitz sequences: theory and applications in the multidimensional case*, Electron. Trans. Numer. Anal. 53 (2020), pp. 113–216.
- [5] B. Beckermann and S. Serra-Capizzano, *On the asymptotic spectrum of finite element matrix sequences*, SIAM J. Numer. Anal. 45 (2007), pp. 746–769.
- [6] A. Böttcher and S.M. Grudsky, *On the condition numbers of large semidefinite Toeplitz matrices*, Linear Algebra Appl. 279 (1998), pp. 285-301.
- [7] A. Böttcher and B. Silbermann, *Introduction to large truncated Toeplitz matrices*. Universitext. Springer-Verlag, New York (1999).
- [8] P. Ciarlet, *The Finite Element Method for Elliptic Problems*. North Holland, Amsterdam (1978).
- [9] J.A. Cottrell, T.J.R. Hughes, and Y. Bazilevs, *Isogeometric Analysis: toward integration of CAD and FEA*. John Wiley & Sons (2009).
- [10] J.A. Cottrell, A. Reali, Y. Bazilevs, and T.J.R. Hughes, *analysis of structural vibrations*, Comput. Methods Appl. Mech. Engrg. 195.41-43 (2006), pp. 5257–5296.
- [11] F. De Prenter, C.V. Verhoosel, E.H. Van Brummelen, M.G. Larson, and S. Badia, *Stability and Conditioning of Immersed Finite Element Methods: Analysis and Remedies*, Arch. Comput. Methods Eng. 30.6 (2023), pp. 3617-3656.
- [12] M. Donatelli, C. Garoni, C. Manni, S. Serra-Capizzano, and H. Speelers, *Robust and optimal multi-iterative techniques for IgA Galerkin linear systems*, Comput. Methods Appl. Mech. Engrg. 284 (2015), pp. 230–264.
- [13] M. Donatelli, C. Garoni, C. Manni, S. Serra-Capizzano, and H. Speelers, *Spectral analysis and spectral symbol of matrices in isogeometric collocation methods*, Math. Comp. 85.300 (2016), pp. 1639-1680.
- [14] M. Donatelli, M. Mazza, and S. Serra-Capizzano, *Spectral analysis and multigrid methods for finite volume approximations of space-fractional diffusion equations*, SIAM J. Sci. Comput. 40.6 (2018), pp. A4007–A4039.
- [15] M. Donatelli, M. Neytcheva, and S. Serra-Capizzano, *Canonical eigenvalue distribution of multilevel block Toeplitz sequences with non-Hermitian symbols*, Spectral theory, mathematical system theory, evolution equations, differential and difference equations, pp. 269–291, Oper. Theory Adv. Appl., 221, Birkhäuser/Springer Basel AG, Basel, 2012.
- [16] A. Dorostkar, M. Neytcheva, and S. Serra-Capizzano, *Spectral analysis of coupled PDEs and of their Schur complements via generalized locally Toeplitz sequences in 2D*, Comput. Methods Appl. Mech. Engrg. 309 (2016), pp. 74–105.

- [17] M. Dumbser, F. Fambri, I. Furci, M. Mazza, S. Serra-Capizzano, and M. Tavelli, *Staggered discontinuous Galerkin methods for the incompressible Navier-Stokes equations: spectral analysis and computational results*, Numer. Linear Algebra Appl. 25.5 (2018), paper e2151.
- [18] C. Garoni, C. Manni, F. Pelosi, and H. Speleers, *Spectral analysis of matrices resulting from isogeometric immersed methods and trimmed geometries.*, Comput. Methods Appl. Mech. Eng. 400 (2022), paper 115551.
- [19] C. Garoni, M. Mazza, and S. Serra-Capizzano, *Block generalized locally Toeplitz sequences: From the theory to the applications*, Axioms 7.3 (2018), paper 49.
- [20] C. Garoni and S. Serra-Capizzano, *Generalized Locally Toeplitz sequences: theory and applications - Vol I*. Springer - Springer Monographs in Mathematics, New York (2017).
- [21] C. Garoni and S. Serra-Capizzano, *Generalized Locally Toeplitz sequences: theory and applications - Vol II*. Springer - Springer Monographs in Mathematics, New York (2018).
- [22] C. Garoni, S. Serra-Capizzano, and D. Sesana, *Spectral analysis and spectral symbol of d -variate Q_p Lagrangian FEM stiffness matrices*, SIAM J. Matrix Anal. Appl. 36.3 (2015), pp. 1100–1128.
- [23] C. Garoni, H. Speleers, S.-E. Ekström, A. Reali, S. Serra-Capizzano, and T.J.R. Hughes, *Symbol-based analysis of finite element and isogeometric B-spline discretizations of eigenvalue problems: exposition and review*, Arch. Comput. Methods Eng. 26.5 (2019), pp. 1639–1690.
- [24] J. S. Hesthaven and T. Warburton, *Nodal Discontinuous Galerkin Methods. Algorithms, Analysis, and Applications*. Springer-verlag, New York, NY (2008).
- [25] R. Glowinski and Y.A. Kuznetsov, *Distributed Lagrange multipliers based on fictitious domain method for second order elliptic problems*, Comput. Methods Appl. Mech. Eng. 196.8 (2007), pp. 1498-1506.
- [26] C. Jordan, *Cours d'Analyse de l'Ecole Polytechnique: Vol. I*. Gauthier-Villars, Paris, 1909.
- [27] Z. Li and K. Ito, *The Immersed Interface Method: Numerical Solutions of PDEs Involving Interfaces and Irregular Domains*. SIAM, Philadelphia, (2006).
- [28] M. Mazza, C. Manni, A. Ratnani, S. Serra-Capizzano, and H. Speleers, *Isogeometric analysis for 2D and 3D curl-div problems: spectral symbols and fast iterative solvers*, Comput. Methods Appl. Mech. Engrg. 344 (2019), pp. 970–997.
- [29] M. Mazza, A. Ratnani, and S. Serra-Capizzano, *Spectral analysis and spectral symbol for the 2D curl-curl (stabilized) operator with applications to the related iterative solutions*, Math. Comp. 88.317 (2019), pp. 1155–1188.
- [30] G.I. Marchuk, Y.A. Kuznetsov, and A.M. Matsokin, *Fictitious domain and domain decomposition methods*, Soviet J. Numer. Anal. Math. Modelling 1.1 (1986), pp. 3-35.
- [31] M. Mazza, S. Serra-Capizzano, and R. Sormani, *Spectral analysis and preconditioners for two-dimensional Riesz distributed-order space-fractional diffusion equations*, Numer. Linear Algebra Appl. 31.3 (2023), paper e2536.
- [32] E. Ngondiep, S. Serra-Capizzano, and D. Sesana, *Spectral features and asymptotic properties for g -circulants and g -Toeplitz sequences*, SIAM J. Matrix Anal. Appl. 31.4 (2009/10), pp. 1663–1687.
- [33] D. Noutsos, S. Serra-Capizzano, and P. Vassalos, *The conditioning of FD matrix sequences coming from semi-elliptic differential equations*, Linear Algebra Appl. 428.2-3 (2008), pp. 600–624.

- [34] R.I. Rahla, S. Serra-Capizzano, and C. Tablino-Possio, *Spectral analysis of P_k Finite Element matrices in the case of Friedrichs–Keller triangulations via Generalized Locally Toeplitz technology*, Numer. Linear Algebra Appl. 27.4 (2020), paper e2302, 28 pp.
- [35] E.B. Saff and V. Totik, *Logarithmic potentials with external fields*, Appendix B by Thomas Bloom, Grundlehren der mathematischen Wissenschaften [Fundamental Principles of Mathematical Sciences], 316. Springer-Verlag, Berlin, 1997.
- [36] A.J.A. Schiavoni-Piazza and S. Serra-Capizzano, *Distribution results for a special class of matrix sequences: joining approximation theory and asymptotic linear algebra*, Electron. Trans. Numer. Anal. 59 (2023), pp. 1–8.
- [37] A.J.A. Schiavoni-Piazza, D. Meadon, and S. Serra-Capizzano, *The β maps: strong clustering and distribution results on the complex unit circle*, Linear Algebra Appl. 688 (2024), pp. 59–77.
- [38] S. Serra-Capizzano, *On the extreme spectral properties of Toeplitz matrices generated by L^1 functions with several minima/maxima*, BIT 36 (1996), pp. 135–142.
- [39] S. Serra-Capizzano, *On the extreme eigenvalues of Hermitian (block) Toeplitz matrices*, Linear Algebra Appl. 270 (1998), pp. 109–129.
- [40] S. Serra-Capizzano, *Distribution results on the algebra generated by Toeplitz sequences: a finite dimensional approach*, Linear Algebra Appl. 328 (2001), pp. 121–130
- [41] S. Serra-Capizzano, *Generalized locally Toeplitz sequences: spectral analysis and applications to discretized partial differential equations*, Linear Algebra Appl. 366 (2003), pp. 371–402.
- [42] S. Serra-Capizzano, *The GLT class as a generalized Fourier analysis and applications*, Linear Algebra Appl. 419.1 (2006), pp. 180–233.
- [43] J.C. Strikwerda, *Finite Difference Schemes and Partial Differential Equations*. Chapman and Hall, International Thompson Publ., New York, 1989.
- [44] P. Tilli, *Locally Toeplitz matrices: spectral theory and applications*, Linear Algebra Appl. 278 (1998), pp. 91–120.
- [45] P. Tilli, *A note on the spectral distribution of Toeplitz matrices*, Linear Multilin. Algebra 45 (1998), pp. 147–159.
- [46] P. Tilli, *Some results on complex Toeplitz eigenvalues*, J. Math. Anal. Appl. 239.2 (1999), pp. 390–401.
- [47] E.E. Tyrtyshnikov, *A unifying approach to some old and new theorems on distribution and clustering*, Linear Algebra Appl. 232 (1996), pp. 1–43.
- [48] E.E. Tyrtyshnikov and N. Zamarashkin, *Spectra of multilevel Toeplitz matrices: advanced theory via simple matrix relationships*, Linear Algebra Appl. 270 (1998), pp. 15–27.
- [49] P. Vassalos, *Asymptotic results on the condition number of FD matrices approximating semi-elliptic PDEs*, Electron. J. Linear Algebra 34 (2018), pp. 566–581.
- [50] H.K. Versteeg and W. Malalasekera, *An Introduction to Computational Fluid Dynamics: The Finite Volume Method*. Pearson Education, (2007).